been established as playing a pivotal role in regulation of fear, emotion and cognition (8,9), has been suggested to be involved in energy regulation because lesion of the amygdala has been reported to induce hyperphagia, resulting in marked obesity (10,11). Moreover, the amygdala has recently been demonstrated to be one of the brain regions regulating appetite via activation of the melanocortin system (12).

Memory formation involves long-term structural alterations of synapses, so-called neuronal plasticity involving cellular and molecular mechanisms of synapse formation, neurite outgrowth, and behavioural adaptation (13). Cellular and molecular events involved with neuronal plasticity are under the range of action of neurotrophic factors, including brain-derived neurotrophic factor (BDNF) and neurotrophin-3 (NT-3) (14,15). BDNF and NT-3 act via high-affinity tyrosine kinase receptors, TrkB and TrkC, respectively (16,17). The BDNF system in the brain is demonstrated to have anti-obesity and anti-diabetic effects, as well as to regulate neural modelling and cognitive processes (18–21). Although the actions of NT-3 in the brain on energy regulation are not yet known, BDNF and NT-3 act in opposite directions in neurite outgrowth and neural activities (22,23). Moreover, glucocorticoid is reported to show an opposite effect in the regulation of BDNF and NT-3 expression in the brain (24).

To explore cognition in diet-induced obese (DIO) mice, in the present study, we examined the cognitive behaviour of DIO mice fed high-fat diet (HFD) using fear-conditioning tests involving regulation mainly by the hippocampus and amygdala (25), and also investigated BDNF and NT-3 content and the expression of their receptors, TrkB and TrkC, in the cerebral cortex, hippocampus, amygdala and hypothalamus of DIO mice compared to control mice.

Materials and methods

Animals and diets

Male C57BL/6J mice (6 weeks old) were obtained from Japan SLC, Inc. (Shizuoka, Japan). They were housed under a 12 : 12 h light/dark cycle (lights on 07.00 h) at room temperature (23 ± 1 °C). The animals had *ad lib.* access to water and food. They were randomly divided into two groups: mice fed HFD (DIO: Research Diets, Inc., New Brunswick, NJ, USA; No. D12492: 524 kcal per 100 g) and mice fed control diet (CD: CE-2, CLEA Japan, Inc., Tokyo, Japan: 346.8 kcal per 100 g). Both groups were fed for 16 weeks. Experiments were performed between 13.00 and 15.00 h. All experiments were performed in accordance with the guidelines established by the Institutional Animal Investigation Committee at Kyoto University and the United States National Institutes of Health Guide for the Care and Use of Laboratory Animals. Every effort was made to optimise the comfort and minimise the use of animals.

Blood sampling and analysis of metabolic parameters

Blood samples were taken from the thoracic aorta using a syringe containing heparin sodium and aprotinin. The blood samples were centrifuged at 15,000×g for 2 min, and plasma was separated and stored at −20 °C until assayed. Plasma metabolic parameters were analysed in accordance with a previous study (3).

Fear-conditioning test

The fear-conditioning test was performed as described in a previous study (26). Briefly, training sessions consisted of pairing a neutral stimulus (conditioned stimulus; CS) of a tone and an aversive stimulus (unconditioned stimulus; US) of an electric foot shock. The conditioning chamber was surrounded by a sound-attenuated chest with an observation window. The foot shock was delivered via the grid floor composed of stainless steel rods. The tone was provided by a ventilation fan making a noise of 65 dB. On the first day, each mouse was trained ten times to associate foot shock with the tone, which was presented for 30 s as a conditioned stimulus and a 0.5-mA foot shock for 2 s as an unconditioned stimulus. Mice were then returned to their home cages. Twenty-four hours later, the contextual response and the cued response were observed. To examine the contextual conditioning response, each mouse was placed in the conditioning chamber without the tone for 5 min and freezing behaviour was measured every 1 min. Freezing was defined as the absence of all movement except for respiration. Freezing was monitored continuously by an observer and was recorded on a chart via a switch. Freezing time was summed, and the freezing percentage was calculated per minute. This response mainly depends on the hippocampus. Three hours after termination of the contextual conditioning response, the cued conditioning response was examined by placing each mouse in a new clear plastic cage with the tone for 3 min. Freezing behaviour was measured every 1 min. This response mainly depends on the amygdala.

Jumping–vocalisation response

To compare the responses to foot shock of DIO mice with those of CD mice, the test was performed as described in a previous study (26) with the foot shock box used in the experiment on contextual fear conditioning of CD and DIO mice. Each mouse was placed individually in the box. After a 3-min period of habituation to the test box, shock titrations were continued upwards and downwards in a stepwise manner (0.5 mA for 2 s). Jumping responses to the foot shock were scored as 0–3 and vocalisation responses to the foot shock were scored as 0–3. Response scores 0, 1, 2 and 3 indicate no response, a slight response, a moderate response and a marked response, respectively. Data are presented as the total score of these two responses.

Spontaneous locomotor activity

As described in our previous study (3), spontaneous locomotor activity was measured for 30 min immediately after CD, and DIO mice fed CD and HFD, respectively, for 16 weeks were placed in a new cage.

Elevated plus maze test

This test was performed in accordance with our previous study (27). The elevated plus maze (Muromachi Kikai Co., Ltd., Tokyo, Japan) was constructed of gray Plexiglas and consisted of four arms (length 300 mm, width 60 mm): two closed arms with high gray walls (150 mm high) and two open arms with a small raised lip (3 mm). The maze was elevated to a height of 400 mm above the ground. At least 1 h before the test, mice were transferred to a standby room (20 lux) that was separated from the test room. Experiments were performed between 13.00 and 15.00 h. Each mouse was placed on the center platform facing an open arm to initiate the test session. Mice were allowed to freely explore the apparatus under overhead fluorescent lighting (20 lux) for 5 min. Increased exploration of the relatively open arms is indicative of reduced anxiety-like behaviour in this paradigm. Open/closed arm entries and time spent in the open/closed arms were scored. Arm entries were scored upon entry of the two front paws into the arm.

Table 1. Metabolic Parameters in Control Diet (CD) and Diet-Induced Obese (DIO) Mice.

	CD	DIO
Body weight (g)	34.2 ± 0.8	54.1 ± 1.0**
Glucose (mg/dl)	117 ± 7	190 ± 7**
Insulin (μU/ml)	18.9 ± 3.2	126.0 ± 28.7**
Leptin (ng/ml)	2.2 ± 0.6	42.1 ± 4.5**

Results are presented as the mean ± SEM (n = 14). Significantly different from CD mice in each group: **P < 0.01.

Measurement of BDNF and NT-3 content in the brain

BDNF and NT-3 content in the brain of CD and DIO mice fed CD and HFD, respectively, for 16 weeks was measured in accordance with our previous study (3) using commercially available measurement kits for BDNF (BDNF Emax® ImmunoAssay System: Promega Inc., Madison, WI, USA) and for NT-3 (NT-3 Emax® ImmunoAssay System: Promega Inc. Madison, WI).

Western blot analysis of TrkB and TrkC

Western blotting of full-length TrkB and TrkC in the brain of CD and HFD mice was performed in accordance with our previous study (3). Full-length TrkB and TrkC were detected using rabbit polyclonal anti-TrkB antibody (sc-8316; Santa Cruz Biotechnology, Inc., Santa Cruz, CA, USA) and rabbit polyclonal anti-TrkC antibody (sc-14025; Santa Cruz Biotechnology, Inc.), respectively. Results represent the densitometry data relative to glyceraldehyde 3-phosphate dehydrogenase detected in each sample.

Statistical analysis

All values are provided as the mean ± SEM. Statistical analysis of the data was carried out by ANOVA followed by Dunnett's multiple-range test. $P < 0.05$ was considered statistically significant.

Results

Metabolic parameters in CD and DIO mice

The metabolic parameters in CD and DIO mice are shown in Table 1. The body weight of DIO mice was 1.6 times greater than that in CD mice. Plasma levels of glucose, insulin and leptin in DIO mice were significantly high compared to those in CD mice.

Fear-conditioning response

CD mice exhibited 93% freezing as a result of fear in the first session in the contextual conditioning response, and the freezing percentage gradually decreased during the sessions to reach 60% in the fifth session (Fig. 1). In DIO mice, the freezing percentage of the contextual fear response was significantly lower than that in CD mice in each session (Fig. 1). DIO mice exhibited 64% freezing percentage in the first session of the contextual fear response, and the freezing percentage subsequently decreased during the sessions to 23% in the fifth session (Fig. 1). Similarly, the freezing percentage of the cued fear response in DIO mice was 47% in the first session, which was much lower than the 81% in CD mice, and a significant decrease in freezing percentage of DIO mice was observed over the course of three cued sessions compared to CD mice (Fig. 1).

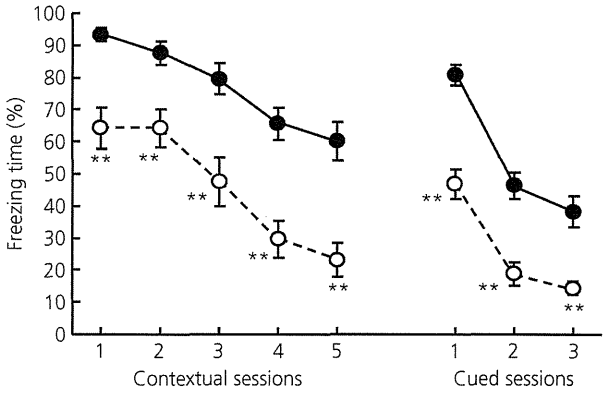

Fig. 1. Fear-conditioning responses in control diet (CD) and diet-induced obese (DIO) mice. Fear-conditioning responses in CD (closed circles) and DIO (open circles) mice. Freezing percentages of CD and DIO mice in the contextual conditioning test were measured every minute for 5 min. Freezing percentages of CD and DIO mice in the cued conditioning test were measured every minute for 3 min. Data points represent the mean ± SEM (n = 9–14). Significantly different from CD mice: *P < 0.05, **P < 0.01.

Jumping-vocalisation test, spontaneous locomotor activity and elevated plus maze test

To compare the sensitivities to foot shock between CD and DIO mice, the jumping-vocalisation test was used. No difference in scores of jumping-vocalisation test was found between CD (score: 3.2 ± 0.3; n = 14) and DIO (score: 2.6 ± 0.1; n = 14) mice. To explore the involvement of motor activity and anxiety in impaired fear-conditioning responses in DIO mice, spontaneous locomotor activity for 30 min after placement of mice into new cages and behaviours in the elevated plus maze test were examined. Spontaneous locomotor activity was not different between CD and DIO mice after 16 weeks of feeding each diet (data not shown). Moreover, both entry times and time spent in the dark and light arms in the elevated plus maze test were not different between CD and DIO mice (data not shown).

BDNF and NT-3 content in the brain areas

BDNF content in the cerebral cortex and hippocampus of DIO mice had significantly decreased to approximately 70% and 60% of CD mice, respectively (Fig. 2A). BDNF content in the amygdala and hypothalamus of DIO mice also tended to decrease compared to that in CD mice (Fig. 2A). By contrast to the changes in BDNF content, NT-3 content in the hippocampus, amygdala and hypothalamus of DIO mice significantly increased to 150%, 165% and 230% of that in CD mice, respectively (Fig. 2B). NT-3 content in the cerebral cortex also tended to be higher than that in CD mice (Fig. 2B).

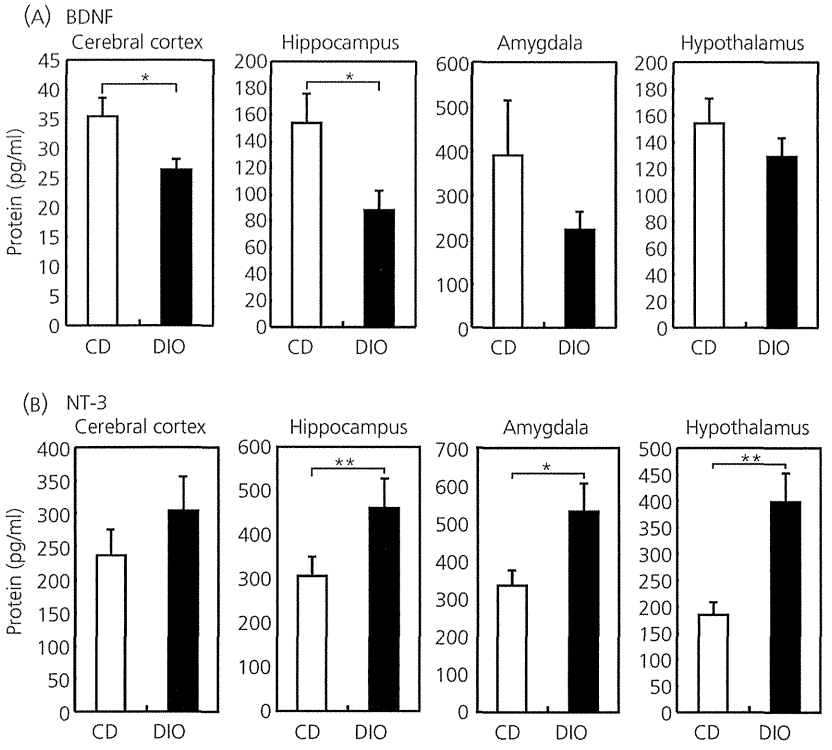

Fig. 2. Content of (A) brain-derived neurotrophic factor (BDNF) and (B) neurotrophin-3 (NT-3) in the cerebral cortex, hippocampus, amygdala and hypothalamus in control diet (CD) and diet-induced obese (DIO) mice. Results are presented as the mean ± SEM (n = 18–29). Significantly different from CD mice: *P < 0.05, **P < 0.01.

Expression of full-length TrkB and TrkC receptors in the brain areas

The expression of full-length TrkB in the amygdala of DIO mice significantly decreased to approximately 70% of CD mice, although not in the cerebral cortex, hippocampus and hypothalamus (Fig. 3A). Full-length TrkC expression in the four brain areas was not significantly different between CD and DIO mice (Fig. 3B).

Discussion

The present study demonstrated that DIO mice showed a significant reduction of both hippocampus-dependent contextual and amygdala-dependent cued fear responses of fear-conditioning test. However, the responses to electric foot shock, locomotor activity and anxiety-like behaviour of DIO mice were the same as those of CD mice. Interestingly, BDNF content in the cerebral cortex and hippocampus of DIO mice was significantly lower than that in CD mice, whereas NT-3 content in the hippocampus, amygdala and hypothalamus of DIO mice was significantly higher than that in CD mice. The expression of full-length TrkB for BDNF in the amygdala of DIO mice significantly decreased compared to that in CD mice, whereas the expression of full-length TrkC for NT-3 in the brain regions was not different between CD and DIO mice. These findings demonstrate that DIO mice display impaired cognition in the fear-conditioning test with an imbalanced interaction between BDNF and NT-3 systems in the cerebral cortex, hippocampus and amygdala related to cognition and fear.

Chronic dietary fat intake, especially saturated fatty acid intake, is reported to contribute to deficits of hippocampus-dependent spatial cognition in the water maze test of rats (5,6,28). The adverse effects of high-dense diets on learning and memory have been associated with impaired hippocampal synaptic plasticity and suppressed neurogenesis (29–31).

Long-term structural alterations of synapses, so-called neuronal plasticity, are regulated by several synaptic molecules including neurotrophic factors, such as BDNF (15), and have been demonstrated to be essential for spatial learning performance, which is dependent primarily on hippocampal functions (15). Animals lacking BDNF show deficits in LTP related to processes of learning and memory, and in hippocampus-dependent spatial learning, which can be amended by exogenous BDNF (15). Although the mechanisms by which a HFD can affect BDNF expression are largely unknown, in the present study, the feeding of HFD or obesity led to a reduction of BDNF content in the hippocampus and cerebral cortex to the extent that cognitive performance was compromised. By contrast to the decrease in BDNF content, the present study demonstrated that NT-3 content was significantly increased in the hippocampus, amygdala and hypothalamus of DIO mice compared to that in CD mice. BDNF and NT-3 oppose one another in regulating

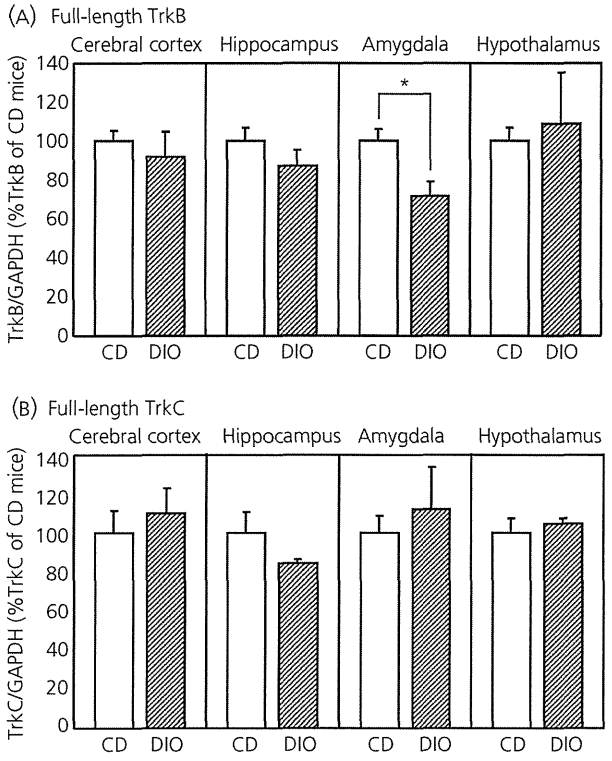

Fig. 3. Expression of full-length TrkB (A) and TrkC (B) in the cerebral cortex, hippocampus, amygdala and hypothalamus in control diet (CD) and diet-induced obese (DIO) mice. Results are presented as the mean ± SEM (n = 3–7). Significantly different from CD mice: *P < 0.05. GAPDH, glyceraldehyde 3-phosphate dehydrogenase.

the dendritic growth of pyramidal neurones in the hippocampus and neural activity (22,23). NT-3 was reported to inhibit the dendritic growth stimulated by BDNF (22). The amygdala, which is well established as playing a pivotal role in regulation of fear, emotion and cognition (8,9), is suggested to be involved in energy regulation because lesion of the amygdala has been reported to induce hyperphasia, resulting in marked obesity (10,11). Moreover, the amygdala has recently been demonstrated to be one of the brain regions regulating appetite via activation of the melanocortin system (12). Taken together, these findings suggest that the impaired fear-conditioning response in DIO mice is attributed to the decrease of BDNF, which facilitates memory processes and the antagonistic actions of NT-3 against BDNF in the hippocampus and amygdala, although the present study did not address the mechanisms responsible for changes in BDNF and NT-3 content in the brain of DIO mice.

Several lines of electrophysiological and behavioural evidence demonstrate that leptin and insulin enhance hippocampal synaptic plasticity and improve learning and memory (31,32). Electrophysiological studies in genetically obese Zucker rats with leptin-receptor deficiency demonstrated that LTP of the hippocampal CA1 region, which is closely related to learning and the formation of memory and is regulated by NMDA and AMPA receptors (6), is markedly impaired compared to lean rats (7). Streptozotocin-treated insulin-deficient rats are reported to exhibit impaired cognition in the water maze test, which is dependent on the hippocampus (33). Therefore, it is likely that impairment of actions of leptin or insulin might be attributable to cognitive deficits in obesity and diabetes mellitus (34,35). Although there is no direct evidence for the impairment of cognition in DIO mice, the impaired cognitive behaviours of fear-conditioning tests observed in the present study may be partly mediated by decreased inherent functions of leptin and insulin in the brain, despite high plasma levels of leptin and insulin, giving rise to the so-called leptin resistance or insulin resistance associated with obesity.

The present study has shown that DIO mice exhibit impairment of both hippocampus-dependent contextual and amygdala-dependent cued responses of the fear-conditioning test. Moreover, BDNF content decreases in the hippocampus and cerebral cortex of DIO mice, whereas NT-3 content increases in the hippocampus, amygdala and hypothalamus of DIO mice, compared to CD mice. The expression of TrkB in the amygdala of DIO mice decreases compared to CD mice. These findings suggest that consumption of a HFD may contribute to aspects of dysfunction in the central nervous system.

Acknowledgements

This work was supported in part by research grants from the Ministry of Education, Culture, Sports, Science and Technology of Japan and the Ministry of Health, Labour and Welfare of Japan. The authors declare that they have no conflicts of interest.

Received 24 November 2011,
revised 27 March 2012,
accepted 4 April 2012

References

1 Elias MF, Elias PK, Sullivan LM, Wolf PA, D'Agostino RB. Lower cognitive function in the presence of obesity and hypertension: the Framingham heart study. *Int J Obes* 2003; **27**: 260–268.
2 Whitmer RA, Gunderson EP, Barrett-Connor E, Quesenberry CP Jr, Yaffe K. Obesity in middle age and future risk of dementia: a 27 year longitudinal population based study. *BMJ* 2005; **330**: 1360–1364.
3 Yamada N, Katsuura G, Ebihara K, Kusakabe T, Hosoda K, Nakao K. Impaired CNS leptin action is implicated in depression associated with obesity. *Endocrinology* 2011; **152**: 2634–2643.
4 Morton GJ, Cummings DE, Baskin DG, Barsh GS, Schwartz MW. Central nervous system control of food intake and body weight. *Nature* 2006; **443**: 289–295.
5 Molteni R, Barnard RJ, Ying Z, Roberts CK, Gómez-Pinilla F. A high-fat, refined sugar diet reduces hippocampal brain-derived neurotrophic factor, neuronal plasticity, and learning. *Neuroscience* 2002; **112**: 803–814.
6 Neves G, Cooke SF, Bliss TV. Synaptic plasticity, memory and the hippocampus: a neural network approach to causality. *Nat Rev Neurosci* 2008; **9**: 65–75.
7 Gerges NZ, Aleisa AM, Alkadhi KA. Impaired long-term potentiation in obese zucker rats: possible involvement of presynaptic mechanism. *Neuroscience* 2003; **120**: 535–539.
8 Weiskrantz L. Behavioral changes associated with ablations of the amygdaloid complex in monkeys. *J Comp Physiol Psychol* 1956; **49**: 381–391.

9 Fuster JM, Uyeda AA. Reactivity of limbic neurons of the monkey to appetitive and aversive signals. *Electroencephalogr Clin Neurophysiol* 1971; **30**: 281–293.

10 Rollins B, King BM. Amygdala-lesion obesity: what is the role of the various amygdaloid nuclei? *Am J Physiol Regul Integr Comp Physiol* 2000; **279**: R1348–R1356.

11 King BM. Amygdaloid lesion-induced obesity: relation to sexual behavior, olfaction, and the ventromedial hypothalamus. *Am J Physiol Regul Integr Comp Physiol* 2006; **291**: R1201–R1214.

12 Boghossian S, Park M, York DA. Melanocortin activity in the amygdala controls appetite for dietary fat. *Am J Physiol Regul Integr Comp Physiol* 2010; **298**: R385–R393.

13 Burns ME, Augustine GJ. Synaptic structure and function: dynamic organization yields architectural precision. *Cell* 1995; **83**: 187–194.

14 Poo MM. Neurotrophins as a synaptic modulator. *Nat Rev Neurosci* 2001; **2**: 24–32.

15 Korte M, Carroll P, Wolf E, Brem G, Thoenen H, Bonhoeffer T. Hippocampal long-term potentiation is impaired in mice lacking brain-derived neurotrophic factor. *Proc Natl Acad Sci USA* 1995; **92**: 8856–8860.

16 Barbacid M. The Trk family of neurotrophin receptors. *J Neurobiol* 1994; **25**: 1386–1403.

17 Patapoutrian A, Reichardt LF. Trk receptors: mediators of neurotrophin action. *Curr Opin Neurobiol* 2001; **11**: 272–280.

18 Tonra JR, Ono M, Liu X, Garcia K, Jackson C, Yancopoulos GD, Wiegand SJ, Wong V. Brain-derived neurotrophic factor improves blood glucose control and alleviates fasting hyperglycemia in C57BLKS-Lepr(db)/lepr(db) mice. *Diabetes* 1999; **48**: 588–594.

19 Nakagawa T, Ogawa Y, Ebihara K, Yamanaka M, Tsuchida A, Taiji M, Noguchi H, Nakao K. Anti-obesity and anti-diabetic effects of brain-derived neurotrophic factor in rodent models of leptin resistance. *Int J Obes Relat Metab Disord* 2003; **27**: 557–565.

20 Musumeci G, Minichiello L. BDNF-TrkB signalling in fear learning: from genetics to neural networks. *Rev Neurosci* 2011; **22**: 303–315.

21 Malcangio M, Lessmann V. A common thread for pain and memory synapses? Brain-derived neurotrophic factor and trkB receptors. *Trends Pharmacol Sci* 2003; **24**: 116–1121.

22 McAllister AK, Katz LC, Lo DC. Opposing roles for endogenous BDNF and NT-3 in regulating cortical dendrite growth. *Neuron* 1997; **18**: 767–778.

23 Adamson CL, Reid MA, Davis RL. Opposite actions of brain-derived neurotrophic factor and neurotrophin-3 on firing features and ion channel composition of murine spiral ganglion neurons. *J Neurosci* 2002; **22**: 1385–1396.

24 Smith MA, Makino S, Kvetnansky R, Post RM. Stress and glucocorticoids affect the expression of brain-derived neurotrophic factor and neurotrophin-3 mRNAs in the hippocampus. *J Neurosci* 1995; **15**: 1768–1777.

25 Kim JJ, Jung MW. Neural circuits and mechanisms involved in Pavlovian fear conditioning: a critical review. *Neurosci Biobehav Rev* 2006; **30**: 188–202.

26 Weeber EJ, Atkins CM, Selcher JC, Varga AW, Mirnikjoo B, Paylor R, Leitges M, Sweatt JD. A role for the β isoform of protein kinase C in fear conditioning. *J Neurosci* 2000; **20**: 5906–5914.

27 Asakawa A, Inui A, Kaga T, Yuzuriha H, Nagata T, Fujimiya M, Katsuura G, Makino S, Fujino MA, Kasuga M. A role of ghrelin in neuroendocrine and behavioral responses to stress in mice. *Neuroendocrinology* 2001; **74**: 143–147.

28 Kaplan RJ, Greenwood CE. Dietary saturated fatty acids and brain function. *Neurochem Res* 1998; **23**: 615–626.

29 Greenwood CE, Winocur G. Learning and memory impairment in rats fed a high saturated fat diet. *Behav Neural Biol* 1990; **53**: 74–87.

30 Lindqvist A, Mohapel P, Bouter B, Frielingsdorf H, Pizzo D, Brundin P, Erlanson-Albertsson C. High-fat diet impairs hippocampal neurogenesis in male rats. *Eur J Neurol* 2006; **13**: 1385–1388.

31 Farr SA, Yamada KA, Butterfield DA, Abdul HM, Xu L, Miller NE, Banks WA, Morley JE. Obesity and hypertriglyceridemia produce cognitive impairment. *Endocrinology* 2008; **149**: 2628–2636.

32 Wickelgren I. Tracking insulin to the mind. *Science* 1998; **280**: 517–519.

33 Gispen WH, Biessels GJ. Cognition and synaptic plasticity in diabetes mellitus. *Trends Neurosci* 2000; **23**: 542–549.

34 Greenwood CE, Winocur G. High-fat diets, insulin resistance and declining cognitive function. *Neurobiol Aging* 2005; **265**: S42–S45.

35 Myers MG, Cowley MA, Münzberg H. Mechanisms of leptin action and leptin resistance. *Annu Rev Physiol* 2008; **70**: 537–556.

Amylin improves the effect of leptin on insulin sensitivity in leptin-resistant diet-induced obese mice

Toru Kusakabe, Ken Ebihara, Takeru Sakai, Licht Miyamoto, Daisuke Aotani, Yuji Yamamoto, Sachiko Yamamoto-Kataoka, Megumi Aizawa-Abe, Junji Fujikura, Kiminori Hosoda and Kazuwa Nakao

Am J Physiol Endocrinol Metab 302:E924-E931, 2012. First published 24 January 2012;
doi: 10.1152/ajpendo.00198.2011

Am J Physiol Endocrinol Metab 302: E924–E931, 2012.
First published January 24, 2012; doi:10.1152/ajpendo.00198.2011.

Amylin improves the effect of leptin on insulin sensitivity in leptin-resistant diet-induced obese mice

Toru Kusakabe,[1] Ken Ebihara,[1,2] Takeru Sakai,[1] Licht Miyamoto,[1] Daisuke Aotani,[1] Yuji Yamamoto,[1] Sachiko Yamamoto-Kataoka,[1] Megumi Aizawa-Abe,[2] Junji Fujikura,[1] Kiminori Hosoda,[1,2] and Kazuwa Nakao[1]

[1]*Department of Medicine and Clinical Science, Kyoto University Graduate School of Medicine; and* [2]*Translational Research Center, Kyoto University Hospital, Kyoto, Japan*

Submitted 25 April 2011; accepted in final form 19 January 2012

Kusakabe T, Ebihara K, Sakai T, Miyamoto L, Aotani D, Yamamoto Y, Yamamoto-Kataoka S, Aizawa-Abe M, Fujikura J, Hosoda K, Nakao K. Amylin improves the effect of leptin on insulin sensitivity in leptin-resistant diet-induced obese mice. *Am J Physiol Endocrinol Metab* 302: E924–E931, 2012. First published January 24, 2012; doi:10.1152/ajpendo.00198.2011.—Leptin enhances insulin sensitivity in addition to reducing food intake and body weight. Recently, amylin, a pancreatic β-cell-derived hormone, was shown to restore a weight-reducing effect of leptin in leptin-resistant diet-induced obesity. However, whether amylin improves the effect of leptin on insulin sensitivity in diet-induced obesity is unclear. Diet-induced obese (DIO) mice were infused with either saline (S), leptin (L; 500 $\mu g \cdot kg^{-1} \cdot day^{-1}$), amylin (A; 100 $\mu g \cdot kg^{-1} \cdot day^{-1}$), or leptin plus amylin (L/A) for 14 days using osmotic minipumps. Food intake, body weight, metabolic parameters, tissue triglyceride content, and AMP-activated protein kinase (AMPK) activity were examined. Pair-feeding and weight-matched calorie restriction experiments were performed to assess the influence of food intake and body weight reduction. Continuous L/A coadministration significantly reduced food intake, increased energy expenditure, and reduced body weight, whereas administration of L or A alone had no effects. L/A coadministration did not affect blood glucose levels during ad libitum feeding but decreased plasma insulin levels significantly (by 48%), suggesting the enhancement of insulin sensitivity. Insulin tolerance test actually showed the increased effect of insulin in L/A-treated mice. In addition, L/A coadministration significantly decreased tissue triglyceride content and increased AMPKα2 activity in skeletal muscle (by 67%). L/A coadministration enhanced insulin sensitivity more than pair-feeding and weight-matched calorie restriction. In conclusion, this study demonstrates the beneficial effect of L/A coadministration on glucose and lipid metabolism in DIO mice, indicating the possible clinical usefulness of L/A coadministration as a new antidiabetic treatment in obesity-associated diabetes.

obesity; diabetes; adenosine 5′-monophosphate-activated protein kinase

LEPTIN, AN ADIPOCYTE-DERIVED HORMONE, has a weight-reducing effect accompanied by reduction in food intake and increase in energy expenditure (11, 13). In general, in rodent models of diet-induced obesity and obese human, although leptin levels rise proportionally with adiposity (16, 23), the increased leptin fails to suppress the progression of obesity. Moreover, even high pharmacological doses of leptin have demonstrated only marginal, if any, effects on body weight in diet-induced obese (DIO) rodents and obese humans (8, 15). This leptin ineffectiveness is called leptin resistance.

Recently, it was shown that amylin, a pancreatic β-cell-derived hormone (4), restored a weight-reducing effect of leptin and that leptin/amylin coadministration effectively reduced body weight in DIO rats (34). Moreover, in overweight/obese humans, coadministration of the amylin analog pramlintide and the leptin analog metreleptin induced significantly greater weight loss than either pramlintide or metreleptin alone (32, 34).

Besides the weight-reducing effect, leptin has a wide range of effects, including an antidiabetic effect. We previously generated transgenic skinny mice (LepTg) overexpressing leptin under the control of the liver-specific human serum amyloid P component promoter, whose plasma leptin levels are elevated compared with those of obese human individuals (30). LepTg mice showed increased glucose metabolism. In LepTg mice, we have demonstrated that leptin increases insulin sensitivity with augmentation of liver and skeletal muscle insulin receptor signaling (30). In addition, LepTg mice had reduced tissue triglyceride contents along with increased energy expenditure through activation of AMP-activated protein kinase (AMPK) (37, 38), a key enzyme that mediates the effect of leptin on fatty acid β-oxidation in skeletal muscle (24).

Given the antidiabetic effect of leptin, we have demonstrated that leptin could be an antidiabetic drug for various types of diabetes, such as lipoatrophic, insulin-deficient, and type 2 diabetes, using animal models (7, 18, 25, 28, 29). In addition, we and others confirmed that leptin treatment effectively reduces food intake and improves insulin sensitivity, hyperglycemia, hypertriglyceridemia, and fatty liver in patients with lipoatrophic diabetes (2, 5, 6, 31). However, in DIO rodents and obese humans, the effect of leptin on insulin sensitivity is also attenuated because of leptin resistance (18).

Evidence indicating that leptin can stimulate insulin sensitivity independently of food intake and body weight reduction via central mechanisms has accumulated (9, 14, 17, 27). Amylin also activates multiple central nervous system regions to regulate both energy and glucose homeostasis (19, 21, 22). Therefore, it is possible that leptin and amylin interact with each other in the regulation of glucose metabolism. However, whether amylin improves the effect of leptin on insulin sensitivity in leptin-resistant obese subjects is unclear.

In this study, we demonstrated that leptin/amylin coadministration, unlike administration of leptin or amylin alone, enhances insulin sensitivity in leptin-resistant DIO mice in addition to reducing body weight accompanied by reduction in food intake and increase in energy expenditure, indicating the pos-

Address for reprint requests and other correspondence: K. Ebihara, Dept. of Medicine and Clinical Science, Kyoto University Graduate School of Medicine, 54 Shogoin Kawahara-cho, Sakyo-ku, Kyoto 606-8507, Japan (e-mail: kebihara@kuhp.kyoto-u.ac.jp).

sible clinical usefulness of leptin/amylin coadministration as a new antidiabetic treatment in obesity-associated diabetes.

MATERIALS AND METHODS

Experimental animals. Eight-week-old male C57BL/6J mice were purchased from Japan SLC, Shizuoka, Japan. The mice were caged individually and kept under a 12:12-h light-dark cycle (lights on at 0900). The mice were fed a high-fat diet (D12451, 45% of energy as fat; Research Diets, New Brunswick, NJ) for 5 wk, with free access to water (termed DIO mice), before experiments. Body weight of DIO mice before experiments was significantly heavier than that of control mice fed a standard diet (NMF, 13% of energy as fat; Oriental Yeast, Tokyo, Japan) (32.6 ± 0.5 vs. 26.9 ± 0.4 g, $P < 0.01$). Metabolic characteristics of control and DIO mice are summarized in Table 1. The result of an insulin tolerance test (ITT) showed that DIO mice were insulin resistant compared with control mice. Animal care and all experiments were conducted in accordance with the Guidelines for Animal Experiments of Kyoto University and were approved by the Animal Research Committee, Graduate School of Medicine, Kyoto University.

Leptin and/or amylin infusion experiments. DIO mice were divided into four treatment groups [saline (S), leptin (L), amylin (A), and leptin plus amylin (L/A)] to be counterbalanced for starting body weight and blood glucose level. On *day 0*, all mice were implanted subcutaneously in the midscapular region with two osmotic minipumps (Alzet model 2002; Alza, Palo Alto, CA) containing either saline, leptin (500 $\mu g \cdot kg^{-1} \cdot day^{-1}$; Amgen, Thousand Oaks, CA), or amylin (100 $\mu g \cdot kg^{-1} \cdot day^{-1}$; Bachem, Torrance, CA). High-fat diet feeding was continued during the experiment.

Body weight and food intake. Body weight was measured on *days 0*, *5*, and *10*. Daily food intake was measured before and during the leptin and/or amylin infusion experiment.

Indirect calorimetry. Measurement of oxygen consumption ($\dot{V}O_2$) and carbon dioxide production ($\dot{V}CO_2$) was performed over a period of 48 h, after >72 h of acclimation, using an Oxymax indirect calorimeter (Columbus Instruments, Columbus, OH) on *days 4* and *5* (n = 4/group) for S, L, A, and L/A-treated mice. Respiratory exchange ratio [ratio of CO_2 production to O_2 ($\dot{V}CO_2/O_2$)], which indicates the relative contribution of fat and carbohydrate oxidation to overall metabolism, was calculated and averaged across the 48-h measurement session.

Metabolic variables. Blood was obtained from nonfasted mice between 1500 and 1700 at the end of the experiment. Blood glucose levels were measured by the glucose oxidase method using a reflectance glucometer (MS-GR102; Terumo, Tokyo, Japan). Plasma insulin levels were measured by enzyme immunoassay with an Insulin-EIA kit (Morinaga, Tokyo, Japan). Plasma glucagon levels were measured by enzyme immunoassay with a Glucagon-EIA kit (Yanaihara, Shizuoka, Japan). Plasma leptin levels were measured by an ELISA kit for mouse leptin (Millipore, Billerica, MA). Plasma amylin levels were measured by enzyme immunoassay using a mouse Amylin-EIA kit (Phoenix Pharmaceuticals, Burlingame, CA).

ITT. An ITT was performed on *day 10*. For the ITT, after a 4-h fast, mice were injected with 0.8 mU/g ip human regular insulin (Humulin R; Eli Lilly Japan, Kobe, Japan). Blood was sampled from the tail vein before and 30, 60, and 120 min after the insulin injection. Blood glucose levels were determined as described above. The area under the curve (AUC) during the ITT was calculated in each mouse.

Liver weight and tissue triglyceride content. Liver weight was measured at the end of the experiment. Liver and skeletal muscle triglyceride content were measured as described previously (18). Liver and gastrocnemius muscle were isolated at the end of the experiment and immediately frozen in liquid nitrogen, and lipids were extracted with isopropyl alcohol-heptane (1:1, vol/vol). After the solvent was evaporated, the lipids were resuspended in 99.5% (vol/vol) ethanol, and the triglyceride content was measured using the Triglyceride E-test Wako kit (Wako Pure Chemicals, Osaka, Japan).

Isoform-specific AMPK activity. AMPK activity was determined as described previously (18). Soleus muscles were isolated at the end of the experiment and immediately frozen in liquid nitrogen. To measure isoform-specific AMPKα1 and -α2 activity in soleus muscle, AMPK was immunoprecipitated from muscle lysates (200 μg of protein) with specific antibodies against the α_1- and α_2-subunits (Upstate Cell Signaling Solutions, Lake Placid, NY) bound to Protein A-Sepharose beads, and the kinase activity of the immunoprecipitates was measured using "SAMS" peptide and [γ-^{32}P]ATP.

Pair-feeding and weight-matched calorie restriction experiments. Pair-feeding experiments were performed to assess the influence of food intake reduction. In this experiment, DIO mice (mean body weight 31.2 ± 0.4 g) were divided into three treatment groups [S, saline + pair-fed L/A-treated mice (PF), and L/A] to be counterbalanced for starting body weight and blood glucose level. Saline, leptin, and amylin were infused using two osmotic minipumps, as described above. Pair-fed mice were fed the same amount of food consumed by L/A-treated mice on the previous day at the end of light phase once for 14 days. Body weight was measured on *days 0* and *10*. Weight-matched calorie restriction experiments were performed to assess the influence of body weight reduction. In this experiment, the food consumption of DIO mice (mean body weight 31.7 ± 0.5 g) was restricted to match their body weight to those of L/A-treated mice (weight-matched DIO mice, termed CR mice). CR mice were fed the ~70% amount of food consumed by S-treated mice on the previous day at the end of light phase at once for 14 days. An ITT was performed on *day 10* of these experiments. Liver and gastrocnemius muscle were obtained for triglyceride content measurements at the end of these experiments.

Statistical analyses. Data are expressed as means ± SE. Comparison between or among groups was by Student's t-test or ANOVA with Fisher's protected least significant difference test. $P < 0.05$ was considered statistically significant.

Table 1. *Metabolic characteristics of control and DIO mice*

Variable	Control (n = 6)	DIO (n = 9)
Blood glucose, mg/dl	142.4 ± 5.4	160.4 ± 6.6
Plasma insulin, pg/ml	466.9 ± 99.1	535.0 ± 87.6
AUC in ITT, %/min × 100	77.3 ± 10.5	102.5 ± 5.5*
Liver TG content, mg/g tissue	9.8 ± 0.8	23.6 ± 2.4**
Skeletal muscle TG content, mg/g tissue	5.2 ± 0.7	5.6 ± 1.1

Values are means ± SE. DIO, diet-induced obese; AUC, area under the curve; ITT, insulin tolerance test; TG, triglyceride. Blood glucose, plasma insulin, liver TG content, and skeletal muscle TG content were measured in saline-treated control and DIO mice at the end of the experiment. Blood samples were obtained during ad libitum feeding. AUC in ITT was measured on *day 10*. *$P < 0.05$ and **$P < 0.01$ vs. control mice.

RESULTS

Effect of leptin and/or amylin on food intake, body weight, and energy expenditure in DIO mice. Leptin and amylin were administered for 14 days in DIO mice, using osmotic minipumps. Plasma leptin and amylin levels at the end of the experiment were shown in Table 2. Administration of leptin (500 $\mu g \cdot g^{-1} \cdot day^{-1}$) was adequately effective in control mice fed a standard diet, as shown in our previous report (18), but it had no significant effect on food intake or body weight in DIO mice (Fig. 1, *A* and *B*), indicating that these DIO mice were in the leptin-resistant state. Administration of amylin (100 $\mu g \cdot g^{-1} \cdot day^{-1}$) had no effect on food intake or body weight in mice fed a standard diet (data not shown) or DIO mice (Fig. 1, *A* and *B*). However, L/A coadminis-

Table 2. *Plasma leptin and amylin levels in mice administered leptin and/or amylin*

Variable, ng/ml	Mouse Group			
	S	L	A	L/A
L	28.5 ± 5.6	53.0 ± 5.3*	19.7 ± 4.8	45.1 ± 6.6*†
A	1.7 ± 0.1	1.8 ± 0.2	2.7 ± 0.2**	2.9 ± 0.2**,##

Values are means ± SE for 8–9 mice in each group. S, saline; L, leptin; A, amylin; L/A, leptin + amylin. Plasma L and A levels were measured at the end of the experiment. Blood samples were obtained during ad libitum feeding. *$P < 0.05$ and **$P < 0.01$ vs. S-treated mice; ##$P < 0.01$ vs. L-treated mice; †$P < 0.05$ vs. A-treated mice in L/A-treated mice.

tration significantly reduced cumulative food intake for 10 days by 15.3% in DIO mice compared with saline administration (Fig. 1*A*). Body weight was decreased by 9.2% for 10 days of L/A coadministration (Fig. 1*B*).

To assess the effect of leptin and/or amylin on energy expenditure, indirect calorimetry was performed. L/A coadministration significantly increased $\dot{V}O_2$, a marker of energy expenditure, in both the light and dark phases (Fig. 1*C*). In addition, L/A coadministration significantly decreased respiratory exchange ratio in the dark phase, indicating increased utilization of fat as the fuel source (Fig. 1*D*).

Effect of leptin and/or amylin on glucose metabolism in DIO mice. On *day 14*, there was no difference in blood glucose levels under ad libitum feeding among groups (Fig. 2*A*). On the other hand, L/A coadministration decreased plasma insulin levels significantly, whereas administration of L or A alone did not change plasma insulin levels, compared with saline administration (282.8 ± 69.6 vs. 535.0 ± 87.6 pg/ml, $P < 0.01$), indicating the improvement of insulin sensitivity in L/A-treated mice (Fig. 2*B*). Plasma glucagon levels of DIO mice were significantly higher than that of control mice (106.9 ± 26.0 vs. 45.0 ± 8.0 pg/ml, $P < 0.01$). L/A coadministration tended to suppress plasma glucagon levels, but not significantly (Fig. 2*C*).

To evaluate insulin sensitivity, we performed ITTs. The ITT actually showed greater decrease in glucose levels after insulin injection in L/A-treated mice than in L- or A-treated mice (Fig. 2*D*). Consistent with these findings, the glucose AUC after insulin injection was decreased only in L/A-treated mice (Fig. 2*E*).

Effect of leptin and/or amylin on liver weight, tissue triglyceride content, and AMPK activity in skeletal muscle in DIO mice. Because fat accumulation in insulin target tissues is considered to be one of the reasons for insulin resistance (36, 41), we examined liver and gastrocnemius muscle triglyceride

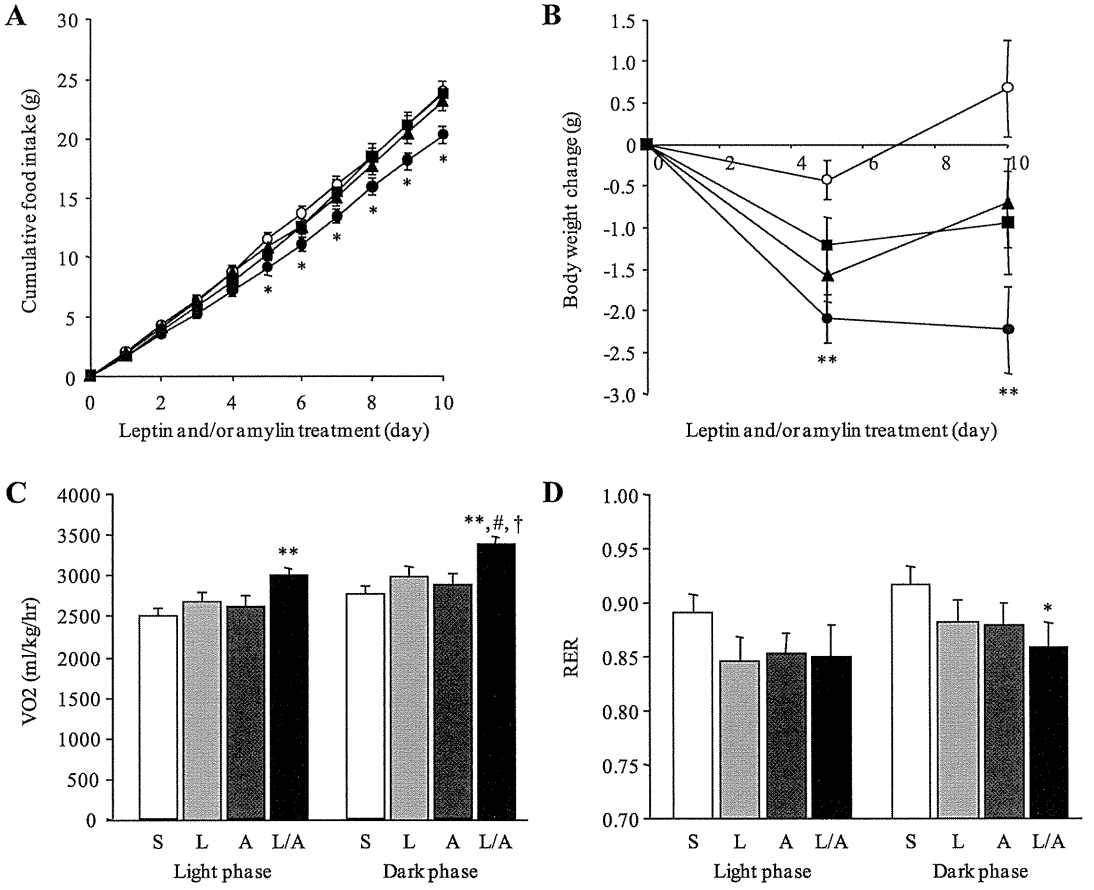

Fig. 1. Effect of leptin and/or amylin on food intake, body weight, energy expenditure, and respiratory exchange ratio (RER) in diet-induced obese (DIO) mice. Cumulative food intake (*A*) and change in body weight (*B*) during the treatment in saline- (S; ○), leptin- (L; ■), amylin- (A; ▲), and leptin + amylin (L/A)-treated mice (●). Values are means ± SE (n = 8–9/group). Oxygen consumption ($\dot{V}O_2$; *C*) and RER (*D*) during the treatment in S-, L-, A-, and L/A-treated mice. Values are means ± SE (n = 4/group). *$P < 0.05$ and **$P < 0.01$ vs. S-treated mice; #$P < 0.05$ vs. L-treated mice; †$P < 0.05$ vs. A-treated mice.

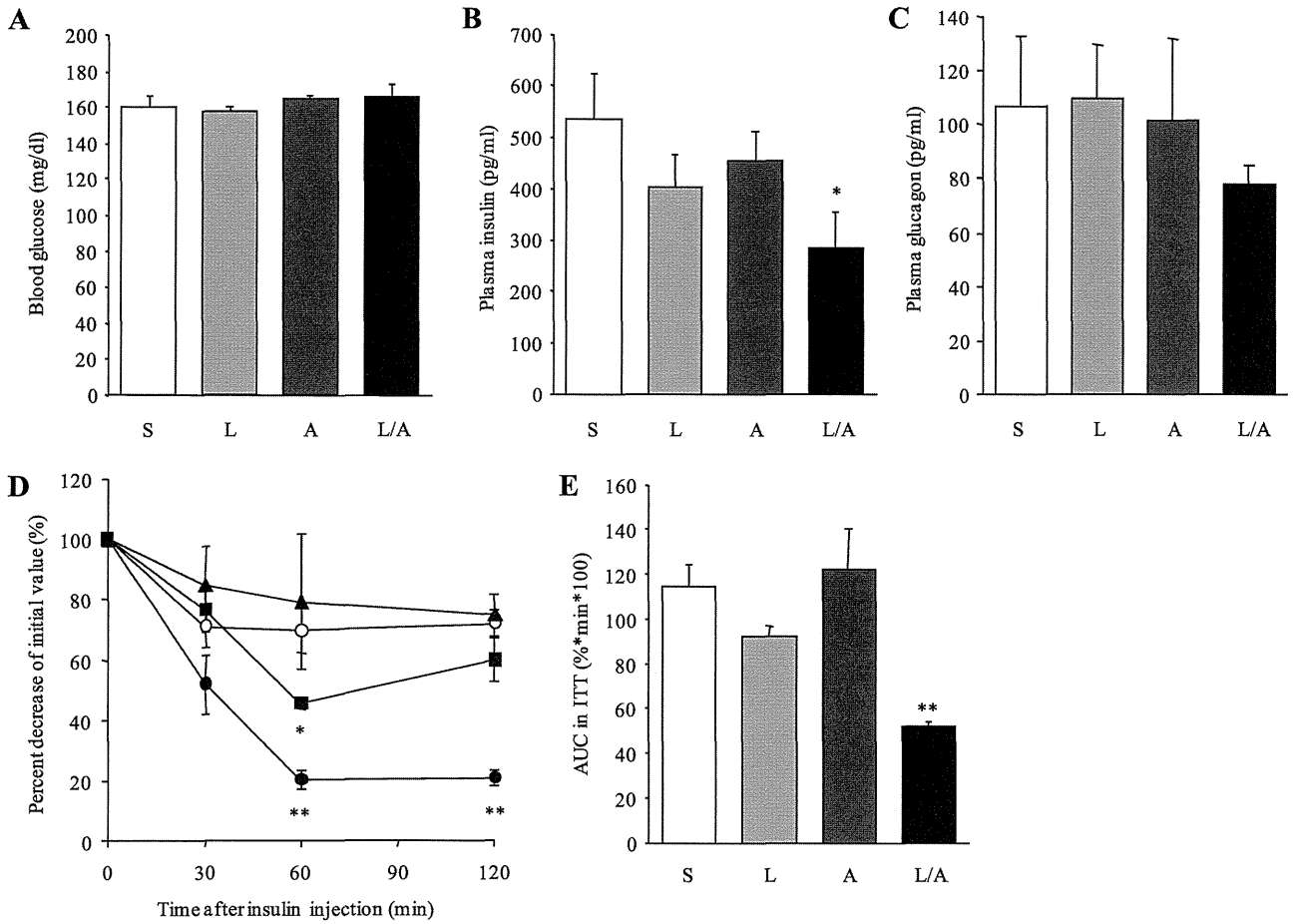

Fig. 2. Effect of L and/or A on glucose metabolism in DIO mice. Blood glucose (*A*), plasma insulin (*B*), and plasma glucagon levels (*C*) under ad libitum feeding on *day 14* in S, L, A, and L/A-treated mice. Values are means ± SE (n = 8–9/group). %Change of initial value of blood glucose levels (*D*) and area under the curve (AUC; *E*) during the insulin tolerance test (ITT) on *day 10* in S (○), L (■), A (▲), and L/A-treated mice (●). Values are means ± SE (n = 4/group). $^{*}P < 0.05$ and $^{**}P < 0.01$ vs. S-treated mice.

contents. Liver weight was significantly decreased (by 16%) in L/A-treated mice compared with that in S-treated mice (Fig. 3*A*). In addition, L/A coadministration significantly decreased triglyceride contents in liver (by 42%) and skeletal muscle (by 46%), whereas administration of L or A alone did not decrease tissue triglyceride contents compared with saline administration (Fig. 3, *B* and *C*).

Leptin has been shown to decrease skeletal muscle triglyceride content in part by increasing fatty acid β-oxidation through AMPKα2 activation in skeletal muscle (24). Therefore, we measured AMPK activity in soleus muscle, where the effect of leptin on AMPK activation was pronounced (24). AMPKα1 activity in soleus muscle was not changed significantly in any group of mice compared with S-treated mice (Fig. 3*D*). On the other hand, AMPKα2 activity in soleus muscle was increased significantly only in L/A-treated mice (by 71%) compared with those in S-treated mice (Fig. 3*E*), consistent with the results of tissue triglyceride contents.

Pair-feeding and weight-matched calorie restriction experiments. We performed pair-feeding experiments to assess whether the body weight reduction and the enhancement of insulin sensitivity by L/A coadministration was associated with food intake reduction. Pair-feeding to L/A-treated mice reduced body weight in DIO mice significantly, but the change was apparently smaller than in L/A-treated mice (Fig. 4*A*). In addition, PF mice showed neither the improvement in insulin sensitivity (Fig. 4, *B* and *C*) nor the decrease in triglyceride contents of liver and skeletal muscle (Fig. 4, *D* and *E*), in contrast to L/A-treated mice.

Then, we performed weight-matched calorie restriction experiments to assess whether the enhancement of insulin sensitivity by L/A coadministration was associated with body weight reduction. To match the body weight to L/A-treated mice, the food intake was restricted to 70% of S-treated mice in CR mice (Fig. 4*A*). In this condition, CR mice showed neither the improvement of insulin sensitivity (Fig. 4, *B* and *C*) nor the decrease in triglyceride contents of liver and skeletal muscle (Fig. 4, *D* and *E*), in contrast to L/A-treated mice.

DISCUSSION

Leptin could be an ideal drug for obesity-associated diabetes because it has both a weight-reducing effect and an antidiabetic effect. However, even high pharmacological doses of leptin elicit only marginal weight loss in non-leptin-deficient DIO rodents and humans (8, 15), whereas leptin replacement ther-

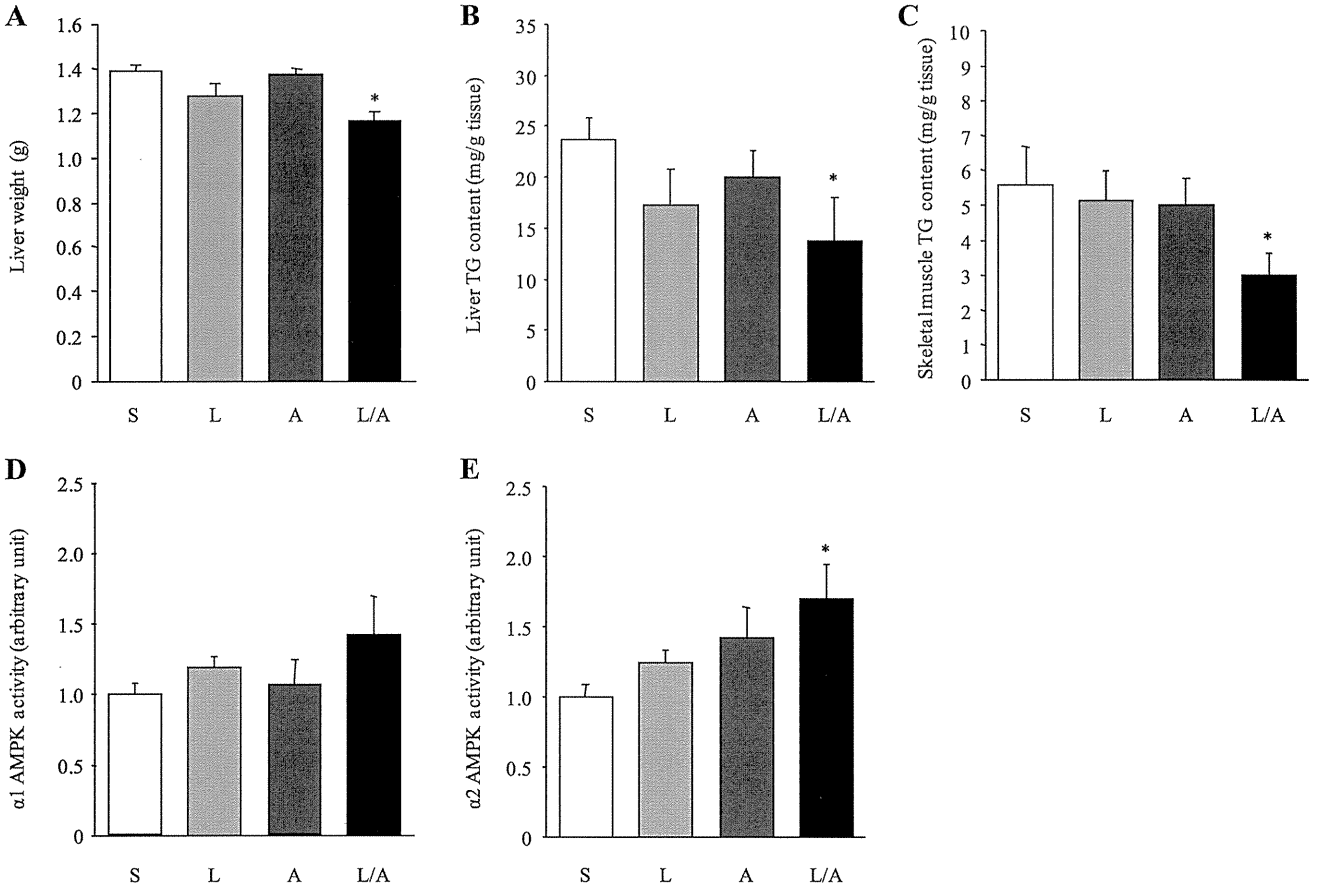

Fig. 3. Effect of L and/or A on tissue triglyceride (TG) content and skeletal muscle AMP-activated protein kinase (AMPK) activity in DIO mice. Liver size (*A*) and liver (*B*) and gastrocnemius muscle (*C*) TG contents on *day 14* in S, L, A, and L/A-treated mice. AMPKα1 (*D*) and AMPKα2 activity (*E*) on *day 14* in soleus muscle of S, L, A, and L/A-treated mice. Values are means ± SE (n = 8–9/group). *$P < 0.05$ vs. S-treated mice.

apy induces profound weight loss in leptin-deficient mice and humans (10, 13). The obese state is thus thought to be associated with leptin resistance, wherein overweight/obese individuals become insensitive to high circulating leptin levels. Sensitizing agents of leptin's effects are expected to treat obesity-associated diabetes comprehensively. In this study, we demonstrated that L/A coadministration not only reduced food intake and body weight but also enhanced insulin sensitivity accompanied by an increase of AMPKα2 activity in skeletal muscle and decrease of tissue triglyceride contents in leptin-resistant DIO mice. Our results indicate the possible clinical usefulness of L/A coadministration as a new antidiabetic treatment in obesity-associated diabetes.

Recently, coadministration of L (500 $\mu g \cdot kg^{-1} \cdot day^{-1}$) and A (100 $\mu g \cdot kg^{-1} \cdot day^{-1}$) was shown to result in a synergistic fat-specific body weight reduction in DIO rats (34). The synergistic antiobesity effect of leptin and amylin was established by the response surface methodology analysis using lower dose ranges of L (0–125 $\mu g \cdot kg^{-1} \cdot day^{-1}$) and A (0–50 $\mu g \cdot kg^{-1} \cdot day^{-1}$) in DIO rats (39). However, because the study of L/A coadministration was not fully examined in mice, the adequate doses of L and A were unclear in DIO mice. Therefore, we chose L (500 $\mu g \cdot kg^{-1} \cdot day^{-1}$) and A (100 $\mu g \cdot kg^{-1} \cdot day^{-1}$) in the present study according to the first report (34). Administration of L (500 $\mu g \cdot g^{-1} \cdot day^{-1}$) had no significant effect on food intake or body weight in DIO mice (Fig. 1, *A* and *B*). Although amylin itself has been shown to dose-dependently reduce food intake and body weight (20, 26), administration of A (100 $\mu g \cdot kg^{-1} \cdot day^{-1}$) was not effective in our DIO mice (Fig. 1, *A* and *B*). Under these conditions, L/A coadministration reduced food intake and body weight in DIO mice in a greater than mathematically additive manner (Fig. 1, *A* and *B*). Our data support that L/A coadministration is a useful treatment for obesity beyond species difference. With the dose of leptin used in the present study, the plasma leptin level in DIO mice increased to 45.1–53.0 ng/ml (Table 2), which can be seen in human obese subjects. In addition, higher leptin levels were obtained in the obese human clinical trial without any clinically significant adverse effects on major organ systems (15). Therefore, the leptin level achieved with the dose used in the present study could be clinically applied in humans.

In general, amylin is considered not to affect insulin secretion and insulin sensitivity but rather to complement the effects of insulin on circulating glucose levels through two main mechanisms (43). First, amylin suppresses postprandial glucagon secretion, thereby decreasing glucagon-stimulated hepatic glucose output following nutrient ingestion (12). Second, amylin also slows the rate of gastric emptying and thus the rate at which nutrients are delivered from the stomach to the small intestine for absorption (44, 45). On the other hand, leptin is

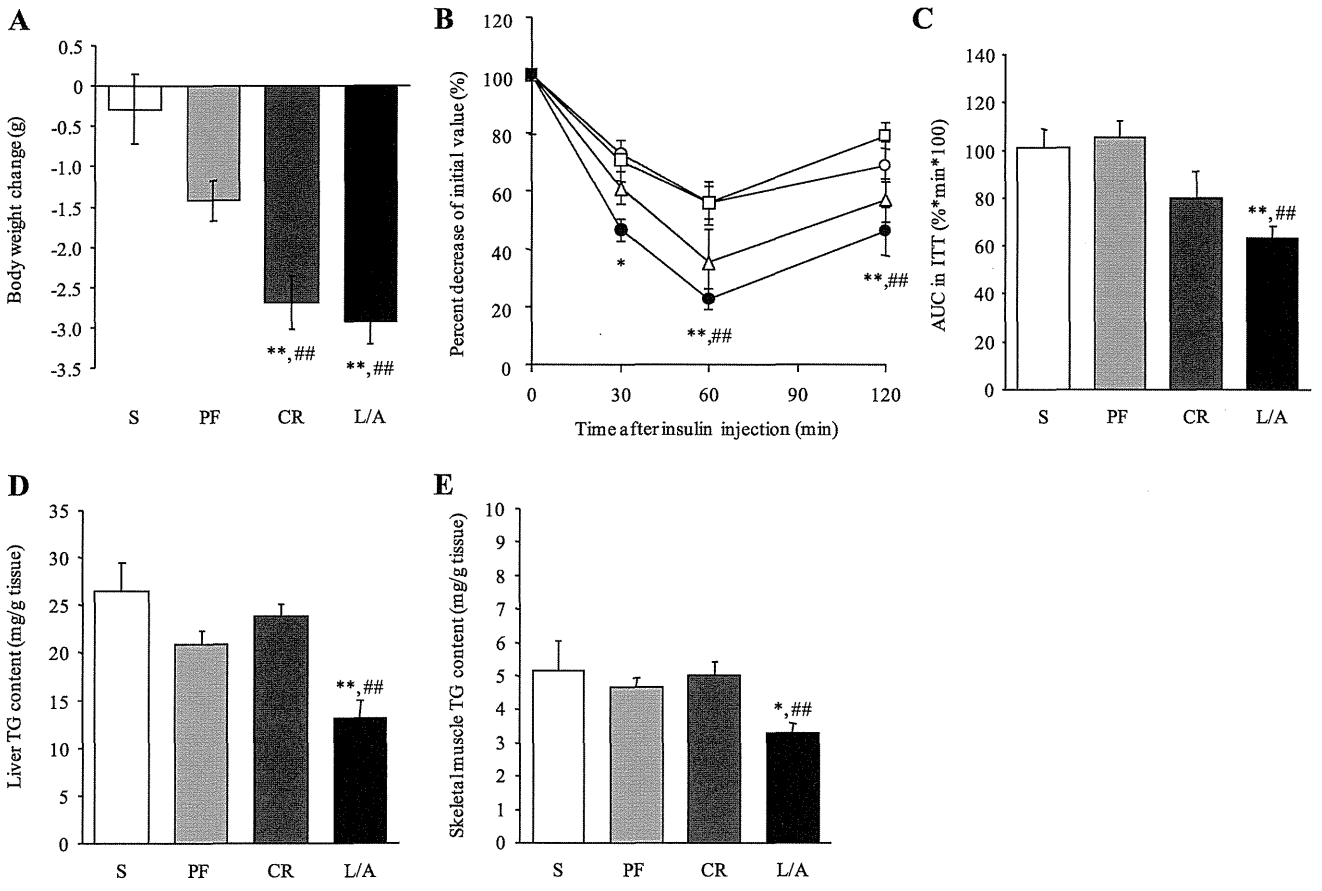

Fig. 4. Pair-feeding and weight-matched calorie restriction experiments. *A*: change in body weight on *day 10* in S, saline + pair-fed L/A-treated (PF), weight-matched DIO (CR), and L/A-treated mice. %Decrease of initial value of blood glucose levels (*B*) and AUC (*C*) during the ITT on *day 10* in S (○), PF (□), CR (△), and L/A-treated mice (●). Liver (*D*) and gastrocnemius muscle (*E*) TG contents on *day 14* in S, PF, CR, and L/A-treated mice. Values are means ± SE (n = 7–12/group). *$P < 0.05$ and **$P < 0.01$ vs. S-treated mice; ##$P < 0.01$ vs. PF mice.

considered to increase insulin sensitivity with augmentation of insulin receptor signaling in insulin target organs such as the liver and skeletal muscle (30) and suppress secretion of glucagon (28, 42). In this study, the tendency toward a decrease, but not a significant one, in plasma glucagon levels was observed in L/A-treated mice (Fig. 2*C*). Further studies are needed to evaluate the effect of leptin on plasma glucagon in DIO mice. Administration of L or A alone did not affect insulin sensitivity in DIO mice (Fig. 2, *A–D*). However, L/A coadministration effectively enhanced insulin sensitivity in DIO mice (Fig. 2, *A–D*). Taken together, our results indicate that amylin improved the insulin-sensitizing action of leptin in DIO mice.

One of the mechanisms by which leptin enhances insulin sensitivity is the reduction of fat accumulation in insulin target organs by activation of the AMPKα2 in skeletal muscle (24, 37, 38). In this study, we demonstrated that only L/A coadministration significantly reduced liver and skeletal muscle triglyceride contents accompanied by AMPKα2 activation in the skeletal muscle (Fig. 3, *A–E*). Previously, we demonstrated that AMPK in skeletal muscle was activated and insulin sensitivity enhanced in LepTg mice. High-fat diet feeding diminished both the activation of AMPK and the enhancement of insulin sensitivity, and diet substitution to standard diet restored them in LepTg mice, indicating that AMPK activity in skeletal muscle closely parallels insulin sensitivity (37). Based on the results of LepTg mice, we proposed that the AMPK activity in peripheral tissues could be a novel biochemical marker of leptin sensitivity in vivo (37). Therefore, the increase of AMPK activity in L/A-treated mice suggests that amylin improved leptin sensitivity in leptin-resistant DIO mice.

For the treatment of obesity-associated diabetes, it is universally accepted that dietary management is used initially with specific emphasis on weight reduction, because weight reduction leads to improvement in deteriorated glucose metabolism (1, 3). Therefore, to assess the influence of food intake and body weight reduction, we compared insulin sensitivity and tissue triglyceride contents among PF, CR, and L/A-treated mice. In this study, PF mice did not show reduced body weight compared with L/A-treated mice (Fig. 4*A*). Because amylin-induced weight loss was attributable primarily to reduced food intake (20, 33, 35), weight loss in L/A-treated mice suggests additional mechanisms such as restoration of leptin's effect on energy expenditure. In previous analyses of calorie restriction effects on metabolism, calorie restriction was accompanied by an expected counterregulatory decline in energy expenditure in rodents (39). However, in this study, we showed that L/A coadministration increased energy expenditure significantly,

whereas it reduced food intake (Fig. 1*C*). In addition, CR mice, whose food consumption was restricted to match their body weight to those of the L/A-treated mice, showed neither the improvement of insulin sensitivity (Fig. 4, *B* and *C*) nor the decrease in liver and skeletal muscle triglyceride contents (Fig. 4, *D* and *E*). These results showed that the improvement of insulin sensitivity and the decrease in tissue triglyceride contents by L/A coadministration were achieved by other mechanisms besides calorie restriction.

In conclusion, we demonstrated that L/A coadministration effectively improves insulin sensitivity in addition to reducing food intake and body weight in DIO mice. Our data indicate that L/A coadministration could be a new antidiabetic treatment in obesity-associated diabetes.

ACKNOWLEDGMENTS

We thank Mayumi Nagamoto, Kyoto University Graduate School of Medicine, for technical assistance and Yoko Koyama, Kyoto University Graduate School of Medicine, for secretarial assistance.

GRANTS

This work was supported in part by research grants from the Ministry of Education, Culture, Sports, Science, and Technology of Japan, the Ministry of Health, Labor, and Welfare of Japan, the Japan Foundation for Applied Enzymology, and the Fujiwara Memorial Foundation.

DISCLOSURES

No conflicts of interest, financial or otherwise, are declared by the authors.

AUTHOR CONTRIBUTIONS

T.K., K.E., and K.N. did the conception and design of the research; T.K., T.S., and L.M. performed the experiments; T.K., T.S., and L.M. analyzed the data; T.K., K.E., T.S., L.M., D.A., Y.Y., S.Y.-K., M.A.-A., J.F., K.H., and K.N. interpreted the results of the experiments; T.K. prepared the figures; T.K. drafted the manuscript; T.K. and K.E. edited and revised the manuscript; T.K., K.E., and K.N. approved the final version of the manuscript.

REFERENCES

1. **Amatruda JM, Richeson JF, Welle SL, Brodows RG, Lockwood DH.** The safety and efficacy of a controlled low-energy ("very-low-calorie") diet in the treatment of non-insulin-dependent diabetes and obesity. *Arch Intern Med* 148: 873–877, 1988.
2. **Beltrand J, Beregszaszi M, Chevenne D, Sebag G, De Kerdanet M, Huet F, Polak M, Tubiana-Rufi N, Lacombe D, De Paoli AM, Levy-Marchal C.** Metabolic correction induced by leptin replacement treatment in young children with Berardinelli-Seip congenital lipoatrophy. *Pediatrics* 120: e291–e296, 2007.
3. **Campfield LA, Smith FJ, Burn P.** Strategies and potential molecular targets for obesity treatment. *Science* 280: 1383–1387, 1998.
4. **Cooper GJ, Leighton B, Dimitriadis GD, Parry-Billings M, Kowalchuk JM, Howland K, Rothbard JB, Willis AC, Reid KB.** Amylin found in amyloid deposits in human type 2 diabetes mellitus may be a hormone that regulates glycogen metabolism in skeletal muscle. *Proc Natl Acad Sci USA* 85: 7763–7766, 1988.
5. **Ebihara K, Kusakabe T, Hirata M, Masuzaki H, Miyanaga F, Kobayashi N, Tanaka T, Chusho H, Miyazawa T, Hayashi T, Hosoda K, Ogawa Y, DePaoli AM, Fukushima M, Nakao K.** Efficacy and safety of leptin-replacement therapy and possible mechanisms of leptin actions in patients with generalized lipodystrophy. *J Clin Endocrinol Metab* 92: 532–541, 2007.
6. **Ebihara K, Masuzaki H, Nakao K.** Long-term leptin-replacement therapy for lipoatrophic diabetes. *N Engl J Med* 351: 615–616, 2004.
7. **Ebihara K, Ogawa Y, Masuzaki H, Shintani M, Miyanaga F, Aizawa-Abe M, Hayashi T, Hosoda K, Inoue G, Yoshimasa Y, Gavrilova O, Reitman ML, Nakao K.** Transgenic overexpression of leptin rescues insulin resistance and diabetes in a mouse model of lipoatrophic diabetes. *Diabetes* 50: 1440–1448, 2001.
8. **El-Haschimi K, Pierroz DD, Hileman SM, Bjørbaek C, Flier JS.** Two defects contribute to hypothalamic leptin resistance in mice with diet-induced obesity. *J Clin Invest* 105: 1827–1832, 2000.
9. **Elmquist JK, Elias CF, Saper CB.** From lesions to leptin: hypothalamic control of food intake and body weight. *Neuron* 22: 221–232, 1999.
10. **Farooqi IS, Jebb SA, Langmack G, Lawrence E, Cheetham CH, Prentice AM, Hughes IA, McCamish MA, O'Rahilly S.** Effects of recombinant leptin therapy in a child with congenital leptin deficiency. *N Engl J Med* 341: 879–884, 1999.
11. **Friedman JM, Halaas JL.** Leptin and the regulation of body weight in mammals. *Nature* 395: 763–770, 1998.
12. **Gedulin BR, Rink TJ, Young AA.** Dose-response for glucagonostatic effect of amylin in rats. *Metabolism* 46: 67–70, 1997.
13. **Halaas JL, Gajiwala KS, Maffei M, Cohen SL, Chait BT, Rabinowitz D, Lallone RL, Burley SK, Friedman JM.** Weight-reducing effects of the plasma protein encoded by the obese gene. *Science* 269: 543–546, 1995.
14. **Hedbacker K, Birsoy K, Wysocki RW, Asilmaz E, Ahima RS, Farooqi IS, Friedman JM.** Antidiabetic effects of IGFBP2, a leptin-regulated gene. *Cell Metab* 11: 11–22, 2010.
15. **Heymsfield SB, Greenberg AS, Fujioka K, Dixon RM, Kushner R, Hunt T, Lubina JA, Patane J, Self B, Hunt P, McCamish M.** Recombinant leptin for weight loss in obese and lean adults: a randomized, controlled, dose-escalation trial. *JAMA* 282: 1568–1575, 1999.
16. **Hosoda K, Masuzaki H, Ogawa Y, Miyawaki T, Hiraoka J, Hanaoka I, Yasuno A, Nomura T, Fujisawa Y, Yoshimasa Y, Nishi S, Yamori Y, Nakao K.** Development of radioimmunoassay for human leptin. *Biochem Biophys Res Commun* 221: 234–239, 1996.
17. **Kamohara S, Burcelin R, Halaas JL, Friedman JM, Charron MJ.** Acute stimulation of glucose metabolism in mice by leptin treatment. *Nature* 389: 374–377, 1997.
18. **Kusakabe T, Tanioka H, Ebihara K, Hirata M, Miyamoto L, Miyanaga F, Hige H, Aotani D, Fujisawa T, Masuzaki H, Hosoda K, Nakao K.** Beneficial effects of leptin on glycaemic and lipid control in a mouse model of type 2 diabetes with increased adiposity induced by streptozotocin and a high-fat diet. *Diabetologia* 52: 675–683, 2009.
19. **Lutz TA.** Amylinergic control of food intake. *Physiol Behav* 89: 465–471, 2006.
20. **Lutz TA, Del Prete E, Scharrer E.** Reduction of food intake in rats by intraperitoneal injection of low doses of amylin. *Physiol Behav* 55: 891–895, 1994.
21. **Lutz TA, Mollet A, Rushing PA, Riediger T, Scharrer E.** The anorectic effect of a chronic peripheral infusion of amylin is abolished in area postrema/nucleus of the solitary tract (AP/NTS) lesioned rats. *Int J Obes Relat Metab Disord* 25: 1005–1011, 2001.
22. **Lutz TA, Senn M, Althaus J, Del Prete E, Ehrensperger F, Scharrer E.** Lesion of the area postrema/nucleus of the solitary tract (AP/NTS) attenuates the anorectic effects of amylin and calcitonin gene-related peptide (CGRP) in rats. *Peptides* 19: 309–317, 1998.
23. **Maffei M, Halaas J, Ravussin E, Pratley RE, Lee GH, Zhang Y, Fei H, Kim S, Lallone R, Ranganathan S, Kern PA, Friedman JM.** Leptin levels in human and rodent: measurement of plasma leptin and ob RNA in obese and weight-reduced subjects. *Nat Med* 1: 1155–1161, 1995.
24. **Minokoshi Y, Kim YB, Peroni OD, Fryer LG, Müller C, Carling D, Kahn BB.** Leptin stimulates fatty-acid oxidation by activating AMP-activated protein kinase. *Nature* 415: 339–343, 2002.
25. **Miyanaga F, Ogawa Y, Ebihara K, Hidaka S, Tanaka T, Hayashi S, Masuzaki H, Nakao K.** Leptin as an adjunct of insulin therapy in insulin-deficient diabetes. *Diabetologia* 46: 1329–1337, 2003.
26. **Morley JE, Flood JF, Horowitz M, Morley PM, Walter MJ.** Modulation of food intake by peripherally administered amylin. *Am J Physiol Regul Integr Comp Physiol* 267: R178–R184, 1994.
27. **Myers MG Jr, Münzberg H, Leinninger GM, Leshan RL.** The geometry of leptin action in the brain: more complicated than a simple ARC. *Cell Metab* 9: 117–123, 2009.
28. **Naito M, Fujikura J, Ebihara K, Miyanaga F, Yokoi H, Kusakabe T, Yamamoto Y, Son C, Mukoyama M, Hosoda K, Nakao K.** Therapeutic impact of leptin on diabetes, diabetic complications, and longevity in insulin-deficient diabetic mice. *Diabetes* 60: 2265–2273, 2011.
29. **Nakao K, Yasoda A, Ebihara K, Hosoda K, Mukoyama M.** Translational research of novel hormones: lessons from animal models and rare human diseases for common human diseases. *J Mol Med* 87: 1029–1039, 2009.

30. **Ogawa Y, Masuzaki H, Hosoda K, Aizawa-Abe M, Suga J, Suda M, Ebihara K, Iwai H, Matsuoka N, Satoh N, Odaka H, Kasuga H, Fujisawa Y, Inoue G, Nishimura H, Yoshimasa Y, Nakao K.** Increased glucose metabolism and insulin sensitivity in transgenic skinny mice overexpressing leptin. *Diabetes* 48: 1822–1829, 1999.
31. **Oral EA, Simha V, Ruiz E, Andewelt A, Premkumar A, Snell P, Wagner AJ, DePaoli AM, Reitman ML, Taylor SI, Gorden P, Garg A.** Leptin-replacement therapy for lipodystrophy. *N Engl J Med* 346: 570–578, 2002.
32. **Ravussin E, Smith SR, Mitchell JA, Shringarpure R, Shan K, Maier H, Koda JE, Weyer C.** Enhanced weight loss with pramlintide/metreleptin: an integrated neurohormonal approach to obesity pharmacotherapy. *Obesity (Silver Spring)* 17: 1736–1743, 2009.
33. **Roth JD, Hughes H, Kendall E, Baron AD, Anderson CM.** Antiobesity effects of the beta-cell hormone amylin in diet-induced obese rats: effects on food intake, body weight, composition, energy expenditure, and gene expression. *Endocrinology* 147: 5855–5864, 2006.
34. **Roth JD, Roland BL, Cole RL, Trevaskis JL, Weyer C, Koda JE, Anderson CM, Parkes DG, Baron AD.** Leptin responsiveness restored by amylin agonism in diet-induced obesity: evidence from nonclinical and clinical studies. *Proc Natl Acad Sci USA* 105: 7257–7262, 2008.
35. **Rushing PA, Hagan MM, Seeley RJ, Lutz TA, Woods SC.** Amylin: a novel action in the brain to reduce body weight. *Endocrinology* 141: 850–853, 2000.
36. **Shulman GI.** Cellular mechanisms of insulin resistance. *J Clin Invest* 106: 171–176, 2000.
37. **Tanaka T, Hidaka S, Masuzaki H, Yasue S, Minokoshi Y, Ebihara K, Chusho H, Ogawa Y, Toyoda T, Sato K, Miyanaga F, Fujimoto M, Tomita T, Kusakabe T, Kobayashi N, Tanioka H, Hayashi T, Hosoda K, Yoshimatsu H, Sakata T, Nakao K.** Skeletal muscle AMP-activated protein kinase phosphorylation parallels metabolic phenotype in leptin transgenic mice under dietary modification. *Diabetes* 54: 2365–2374, 2005.
38. **Tanaka T, Masuzaki H, Yasue S, Ebihara K, Shiuchi T, Ishii T, Arai N, Hirata M, Yamamoto H, Hayashi T, Hosoda K, Minokoshi Y, Nakao K.** Central melanocortin signaling restores skeletal muscle AMP-activated protein kinase phosphorylation in mice fed a high-fat diet. *Cell Metab* 5: 395–402, 2007.
39. **Trevaskis JL, Coffey T, Cole R, Lei C, Wittmer C, Walsh B, Weyer C, Koda J, Baron AD, Parkes DG, Roth JD.** Amylin-mediated restoration of leptin responsiveness in diet-induced obesity: magnitude and mechanisms. *Endocrinology* 149: 5679–5687, 2008.
40. **Turek VF, Trevaskis JL, Levin BE, Dunn-Meynell AA, Irani B, Gu G, Wittmer C, Griffin PS, Vu C, Parkes DG, Roth JD.** Mechanisms of amylin/leptin synergy in rodent models. *Endocrinology* 151: 143–152, 2010.
41. **Unger RH.** Minireview: weapons of lean body mass destruction: the role of ectopic lipids in the metabolic syndrome. *Endocrinology* 144: 5159–5165, 2003.
42. **Wang MY, Chen L, Clark GO, Lee Y, Stevens RD, Ilkayeva OR, Wenner BR, Bain JR, Charron MJ, Newgard CB, Unger RH.** Leptin therapy in insulin-deficient type 1 diabetes. *Proc Natl Acad Sci USA* 107: 4813–4819, 2010.
43. **Weyer C, Maggs DG, Young AA, Kolterman OG.** Amylin replacement with pramlintide as an adjunct to insulin therapy in type 1 and type 2 diabetes mellitus: a physiological approach toward improved metabolic control. *Curr Pharm Des* 7: 1353–1373, 2001.
44. **Young AA, Gedulin B, Vine W, Percy A, Rink TJ.** Gastric emptying is accelerated in diabetic BB rats and is slowed by subcutaneous injections of amylin. *Diabetologia* 38: 642–648, 1995.
45. **Young AA, Gedulin BR, Rink TJ.** Dose-responses for the slowing of gastric emptying in a rodent model by glucagon-like peptide (7–36) NH2, amylin, cholecystokinin, and other possible regulators of nutrient uptake. *Metabolism* 45: 1–3, 1996.

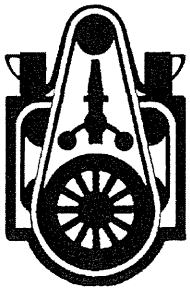

Peritoneal Dialysis International, Vol. 33, pp. 143–154
doi: 10.3747/pdi.2011.00033

0896-8608/13 $3.00 + .00

PERITONEAL FIBROSIS AND HIGH TRANSPORT ARE INDUCED IN MILDLY PRE-INJURED PERITONEUM BY 3,4-DIDEOXYGLUCOSONE-3-ENE IN MICE

Hideki Yokoi,[1] Masato Kasahara,[1] Kiyoshi Mori,[1] Takashige Kuwabara,[1] Naohiro Toda,[1] Ryo Yamada,[2] Shinji Namoto,[2] Takashi Yamamoto,[2] Nana Seki,[2] Nozomi Souma,[2] Taku Yamaguchi,[2] Akira Sugawara,[1] Masashi Mukoyama,[1] and Kazuwa Nakao[1]

Department of Medicine and Clinical Science,[1] Kyoto University Graduate School of Medicine, Kyoto, and Research and Development,[2] JMS Co. Ltd., Hiroshima, Japan

Peritoneal dialysis (PD) solution contains high concentrations of glucose and glucose degradation products (GDPs). One of several GDPs—3,4-dideoxyglucosone-3-ene (3,4-DGE)—was recently identified as the most reactive and toxic GDP in PD fluids. *In vitro,* 3,4-DGE has been shown to induce mesothelial cell damage; however, its role in peritoneal fibrosis *in vivo* remains unclear. In the present study, we intraperitoneally administered chlorhexidine gluconate (CG) for mild peritoneal injury, and we then injected 3,4-DGE [38 μmol/L (low concentration) or 145 μmol/L (high concentration)] 5 times weekly for 4 weeks. Significant thickening of the parietal peritoneal membrane was observed only when treatment with low or high concentrations of 3,4-DGE occurred after CG administration, but not when either CG or 3,4-DGE alone was given. The combination of CG and 3,4-DGE also caused upregulation of messenger RNA expression of transforming growth factor β1, connective tissue growth factor, fibronectin, collagen type 1 α1 chain, alpha smooth muscle actin (α-SMA), vascular endothelial growth factor 164, NADPH oxidase 1 and 4, p22phox, p47phox, and gp91phox in peritoneal tissue. Treatment with CG alone was sufficient to cause significant F4/80-positive macrophage infiltration, appearance of α-SMA–positive cells, and vessel formation in the submesothelial layer. Addition of 3,4-DGE markedly enhanced those changes and induced apoptosis, mainly in leukocytes. The concentration of 3,4-DGE in the abdominal cavity declined more rapidly in CG-treated mice than in PBS-treated mice. Peritoneal membrane permeability determined by peritoneal equilibration test showed high transport conditions in peritoneum treated with both CG and 3,4-DGE. These results indicate that, when mild peritoneal damage is already present, 3,4-DGE causes peritoneal thickening and fibrosis, resulting in deterioration of peritoneal membrane function.

Correspondence to: M. Kasahara, Department of Medicine and Clinical Science, Kyoto University Graduate School of Medicine, 54 Shogoin Kawahara-cho, Sakyo-ku, Kyoto 606-8507 Japan.
kasa@kuhp.kyoto-u.ac.jp
Received 9 February 2011; accepted 9 April 2012

Perit Dial Int 2013; 33(2):143-154 www.PDIConnect.com
epub ahead of print: 01 Nov 2012 doi:10.3747/pdi.2011.00033

KEY WORDS: Peritoneum; mesothelial cells; 3,4-DGE; apoptosis; macrophages; angiogenesis; chlorhexidine gluconate.

Peritoneal dialysis (PD) is a well-established method of home dialysis for patients with end-stage renal failure. During long-term PD, the peritoneal membrane develops peritoneal fibrosis in response to a variety of injuries, including bioincompatible PD solutions, peritonitis, uremia, and chronic inflammation (1,2). Solutions for PD contain high concentrations of glucose, which result in glucose degradation products (GDPs) during the process of heat sterilization. Some GDPs identified in PD fluid (3,4) include acetaldehyde, 3-deoxyglucosone, formaldehyde, 2-furaldehyde, glyoxal, 5-hydroxymethylfurfural, methylglyoxal (MGO), and 3,4-dideoxyglucosone-3-ene (3,4-DGE). Among those GDPs, the highly reactive 3,4-DGE is a toxic substance in PD fluid (4,5). Recently, PD fluid with a neutral pH and lower GDPs has shown improved performance, as indicated by reduced levels of inflammatory markers in effluent and of circulating advanced glycation endproducts (6).

Fluids containing high GDP levels are relevant to peritoneal fibrosis and loss of ultrafiltration (7,8). Although the mechanisms of GDP cytotoxicity are not fully understood, 3,4-DGE has been shown to affect the cytotoxicity of acidic, heat-sterilized PD fluid on human peritoneal mesothelial cells (9). In particular, 3,4-DGE induces apoptosis and epithelial–mesenchymal transition (EMT) in peritoneal mesothelial cells (10). The concentration of 3,4-DGE in conventional PD fluids is normally 10–38 μmol/L (4,5), enough to promote mesothelial cell apoptosis (10). The high reactivity of

3,4-DGE is responsible for depletion of total intracellular glutathione (9), suggesting that 3,4-DGE can enhance oxidative stress in peritoneal mesothelial cells (11). Infusion of conventional PD solution containing an intermediate level of GDPs and lipopolysaccharide (compared with low-GDP solution and lipopolysaccharide) induced high peritoneal transport in rats (12,13). Low-GDP solution caused less peritoneal injury and submesothelial vascularization in rats (14).

Peritoneal dialysis fluid containing GDPs is closely associated with EMT of peritoneal mesothelial cells *in vivo* (15). However, it is not clear whether 3,4-DGE plays a role in peritoneal damage *in vivo,* because no report has shown that 3,4-DGE induces peritoneal fibrosis in that situation. We therefore used two doses of 3,4-DGE—38 μmol/L, the highest found in conventional PD fluid, and 145 μmol/L, higher than the amount found in PD fluid—to examine the role of 3,4-DGE in peritoneal fibrosis and inflammation *in vivo*. We also examined whether pre-existing chlorhexidine gluconate (CG)–induced peritoneal injury increases 3,4-DGE–induced peritoneal injury.

METHODS

ANIMAL MODELS

All animal experiments were approved by the animal experimentation committee of Kyoto University Graduate School of Medicine. Purification of 3,4-DGE was performed as previously described (11). We treated C57BL/6J mice weighing approximately 26 g with intraperitoneal injections of 0.3 mL 0.1% CG in 15% ethanol and 85% phosphate-buffered saline (PBS) every other day for 1 week; they were then injected with 38 μmol/L or 145 μmol/L 3,4-DGE dissolved in 1 mL PBS every weekday for 4 weeks without antibiotics. Control mice received PBS only. Mice were assigned randomly to one of the following groups:

- Group 1: initial PBS and subsequent PBS without 3,4-DGE [PBS+3,4-DGE(−)], $n = 10$
- Group 2: initial PBS and subsequent 38 μmol/L 3,4-DGE (PBS+38 μmol/L 3,4-DGE), $n = 8$
- Group 3: initial PBS and subsequent 145 μmol/L 3,4-DGE (PBS+145 μmol/L 3,4-DGE), $n = 5$
- Group 4: initial CG and subsequent PBS without 3,4-DGE [CG+3,4-DGE(−)], $n = 8$
- Group 5: initial CG and subsequent 38 μmol/L 3,4-DGE (CG+38 μmol/L 3,4-DGE), $n = 11$
- Group 6: initial CG and subsequent 145 μmol/L 3,4-DGE (CG+145 μmol/L 3,4-DGE), $n = 5$

QUANTITATIVE ANALYSIS OF 3,4-DGE IN PLASMA AND PERITONEAL EFFLUENT

The concentration of 3,4-DGE in the abdominal cavity was evaluated. Mice were injected with PBS ($n = 8$) or 0.1% CG ($n = 7$) every other day for 1 week. Then, using an 18G needle, 4 mL 3,4-DGE diluted in PBS was injected into the peritoneal cavity of the mice. Peritoneal solution was collected at 1, 10, 20, and 30 minutes after injection. At 30 minutes after injection, blood samples were collected using heparin-coated capillary tubes from mice given 145 μmol/L 3,4-DGE ($n = 2$ from the PBS group, $n = 3$ from the CG group). Blood samples were centrifuged and plasma components were separated.

The concentrations of 3,4-DGE in plasma and peritoneal effluent were analyzed by liquid chromatography–mass spectrometry as a quinoxaline derivative after a reaction with 2,3-diamino naphthalene. Briefly, 50 μL of sample or standard solution was diluted with an equivalent amount of 0.2 mol/L sodium phosphate buffer (pH 7.4). Then 100 μL of 0.05% 2,3-diamino naphthalene (Tokyo Chemical Industry, Tokyo, Japan) in acetonitrile was added to the solution and carefully mixed. For deproteinization, the mixture was centrifuged (6000*g* for 10 minutes), after which an aliquot of the supernatant was incubated at 25°C for 20 hours under dark conditions for derivative formation. The reaction solution was assayed by reverse-phase high-performance liquid chromatography using a Symmetry column (Waters, Milford, MA, USA) with 25% – 65% gradient elution of acetonitrile containing 0.1% formic acid. The 3,4-DGE-quinoxaline derivative was then detected as protonated molecular ion at 267.1 Da $[C_{16}H_{14}N_2O_2 + H]^+$ by electrospray positive–ionization mass spectrometry.

The preliminary experiment confirmed that the blood component inhibited the reaction between 3,4-DGE and 2,3-diaminonaphthalene, and therefore, to minimize the inhibitory effect, the calibration standards were prepared using serum. For analysis of the peritoneal fluid, aqueous solutions of 3,4-DGE were used as calibration standards. All standard solutions were treated using identical derivatization processing.

MODIFIED PERITONEAL EQUILIBRATION TEST

Before the mice were humanely euthanized, a modified peritoneal equilibration test was performed to determine peritoneal permeability as previously described (16). Briefly, the mice (group 1: $n = 3$; group 2: $n = 3$; group 4: $n = 3$; group 5: $n = 5$) were given 3-mL intraperitoneal injections of 7% glucose dialysis solution (Perisate: JMS, Hiroshima, Japan). After a 2-hour dwell, effluents

were collected and blood samples were drawn. Serum and dialysate creatinine and urea nitrogen levels were measured by the enzymatic method (SRL, Tokyo, Japan). Calculation of the mass transfer-area coefficient (MTAC) of urea was calculated as previously described (17). Mice were euthanized under anesthesia at 5 weeks after CG-treatment, and samples were collected for histologic and biochemical analyses.

HISTOLOGY AND IMMUNOHISTOCHEMICAL STUDY FOR THE PERITONEUM

Anterior abdominal walls containing parietal peritoneum were fixed with 4% buffered paraformaldehyde and embedded in paraffin. We measured the thickness of the fibrotic submesothelial zone above the abdominal muscle layer in cross-sections as previously described (18).

For immunohistochemical analyses of F4/80, CD31, and cytokeratin, the sections were processed as described, with some modifications (18,19). After 0.1% trypsin-mediated antigen retrieval, the samples were incubated with rat monoclonal anti-F4/80 antibody (Serotec, Oxford, UK), rat monoclonal anti-CD31 antibody (BD Biosciences, San Diego, CA, USA), or rabbit polyclonal anti-cytokeratin antibody (Dako, Glostrup, Denmark). After incubation with biotin-conjugated secondary anti-rat immunoglobulin G antibody (Vector Laboratories, Burlingame, CA, USA), the specimens were treated with streptavidin-conjugated horseradish peroxidase (Dako) and then developed using 3,3′-diaminobenzidine tetrahydrochloride (Dako). For immunohistochemical analyses of alpha smooth muscle actin (α-SMA), the sections were processed using microwave-mediated antigen retrieval and were then incubated with rabbit polyclonal anti-α-SMA antibody (Abcam, Cambridge, UK).

REAL-TIME POLYMERASE CHAIN REACTION ANALYSIS

Quantitative real-time polymerase chain reaction was performed using Premix Ex Taq (Takara Bio, Shiga, Japan) on an Applied Biosystems 7300 real-time polymerase chain reaction system (Applied Biosystems, Foster City, CA, USA) or a StepOnePlus system (Applied Biosystems) as previously described, with some modifications (18,19). Gene-specific primers and probes were then used to determine the expression levels of mouse transforming growth factor β1 (TGF-β1), connective tissue growth factor (CTGF), fibronectin, collagen type 1 alpha 1 chain (COL1A1), α-SMA, vascular endothelial growth factor 164 (VEGF164), NADPH oxidase 1 (NOX1) and 4 (NOX4), p22phox, p47phox, and gp91phox (Table 1). Expression

TABLE 1
TaqMan primers and probe sequences[a]

Gene	Forward primer	Reverse primer	Probe
TGF-β1	5′-GACGTCACTGGAGTTGTACGG-3′	5′-GCTGAATCGAAAGCCCTGT-3′	5′-FAM-AGTGGCTGAACCAAGGAGACGGAA-TAMRA-3′
CTGF	5′-TTCCCGAGAAGGGTCAAGCT-3′	5′-TCCTTGGGCTCGTCACACA-3′	5′-FAM-CCTGGGAAATGCTGCAAGGAGTGG-TAMRA-3′
Fibronectin	5′-ATCATTTCATGCCAACCAGTT-3′	5′-TCGCACTGGTAGAAGTTCCA-3′	5′-FAM-CCGACGAAGAGCCCTTACAGTTCCA-TAMRA-3′
COL1A1	5′-GTCCCAACCCCCAAAGAC-3′	5′-CATCTTCTGAGTTTGGTGATACGT-3′	5′-FAM-TGCTGTGCTTTCTGCCCGGA-TAMRA-3′
α-SMA	5′-CCTGACGCTGAAGTATCCGATAG-3′	5′-GGTGCCAGATCTTTTCCATGTC-3′	5′-FAM-ACACGGCATCATCACCAACTGGGA-TAMRA-3′
VEGF164	5′-AACGATGAAGCCCTGGAGTG-3′	5′-GACAAACAAATGCTTTCTCCCG-3′	5′-FAM-CTGTAGGAAGCTCATCTCTCCTATGTGC-TAMRA-3′
NOX1	5′-TCGTCTATATCATCTGCTTAGGGATC-3′	5′-GGCTTTCACCCAAGCTCTCC-3′	5′-FAM-GGCTTTCACCCAAGCTCTCC-TAMRA-3′
NOX4	5′-GCAAGACTCTACACATCACATGTG-3′	5′-,TGCTGCATTCAGTTCAAGGAAATC-3′	5′-FAM-TCTCAGGTGTGCATGTAGCCGCCCA-TAMRA-3′
p22phox	5′-CCCCTCACCAGGAATTACTACG-3′	5′-CACTGCTCACCTCGGATGG-3′	5′-FAM-CTCCACTTCCTGTTGTCGGTGCCTGC-TAMRA-3′
p47phox	5′-GGCGAGATCCACACAGAGAAC-3′	5′-CGTTGAAGTATTCAGTGAGAGTGC-3	5′-FAM-TCCCACACCTCCCGGCACCCAG-TAMRA-3′
gp91phox	5′-GGTGACAATGAGAACGAAGAGTATC-3′	5′-GAGACACAGTGTGATGACAATTCC-3′	5′-FAM-CAGCCAACCGAGTCACGGCCACATAC-TAMRA-3′

TGF-β1 = transforming growth factor β1; CTGF = connective tissue growth factor; COL1A1 = collagen type 1 α1 chain; α-SMA = alpha smooth muscle actin, VEGF = vascular endothelial growth factor; NOX = NADPH oxidase; p22phox = cytochrome b-245, alpha polypeptide; p47phox = neutrophil cytosolic factor 1; gp91phox = cytochrome b245, beta polypeptide.
[a] Purchased from Applied Biosystems and Sigma Genosys, Tokyo, Japan.

of each messenger RNA (mRNA) was normalized to GAPDH mRNA (TaqMan rodent GAPDH control reagents: Applied Biosystems).

ASSESSMENT OF APOPTOSIS

Apoptosis was quantified using a terminal deoxynucleotidyl transferase–mediated dUTP nick end labeling (TUNEL) assay with *in situ* cell death detection kit and fluorescein (Roche, Basel, Switzerland) as previously described (20). To detect apoptotic cell types, triple staining for CD45, TUNEL, and DAPI was performed. Paraffin-embedded peritoneal sections 4 μm in thickness were deparaffinized and treated with microwaves for antigen retrieval. Sections were then processed with rabbit polyclonal anti-CD45 antibody (Abcam) for 1 hour at room temperature. After incubation with DyLight 549 conjugated donkey anti-rabbit antibody (Jackson ImmunoResearch, West Grove, PA, USA), the sections were treated with 0.1% Triton X in 0.1% sodium citrate buffer and then incubated with TUNEL reaction mixture.

STATISTICAL ANALYSIS

Data are expressed as mean ± standard error of the mean. The statistical analysis was performed using one-way analysis of variance or the Student t-test, as appropriate. A p value of less than 0.05 was considered statistically significant.

RESULTS

PRETREATMENT WITH CG ENHANCES 3,4-DGE–INDUCED PERITONEAL FIBROSIS

Mice received intraperitoneal injections of PBS every other day for 1 week (3 times) and then injections of low (38 μmol/L) or high (145 μmol/L) concentrations 3,4-DGE every weekday for 4 weeks. Mice treated with 3,4-DGE or CG (or both) and mice receiving PBS+3,4-DGE(−) all had similar body weights (Figure 1). The thickness of the peritoneal membrane was analyzed using Masson trichrome staining. The PBS+3,4-DGE(−) and 38 μmol/L or 145 μmol/L PBS+3,4-DGE mice showed almost normal peritoneal tissues. Notably, the thickness of the peritoneal membrane was greater for CG+38 μmol/L 3,4-DGE mice than for CG+3,4-DGE(−) mice. The CG+145 μmol/L 3,4-DGE mice showed even more pronounced peritoneal membrane thickness: PBS+3,4-DGE(−), 27.9 ± 4.8 μm; PBS+38 μmol/L 3,4-DGE, 23.5 ± 1.6 μm; PBS+145 μmol/L 3,4-DGE, 26.8 ± 4.1 μm; CG+3,4-DGE(−), 47.2 ± 1.7 μm; CG+38 μmol/L 3,4-DGE, 142 ± 11 μm; CG+145 μmol/L 3,4-DGE, 253 ± 16 μm (Figure 2).

EFFECT OF CG AND 3,4-DGE ON GENE EXPRESSION IN PERITONEAL INJURY

We next examined gene expression of TGF-β1, CTGF, fibronectin, COL1A1, α-SMA, and VEGF164 in peritoneum (Figure 3). Administration of 38 μmol/L or 145 μmol/L 3,4-DGE in PBS-treated mice did not increase mRNA expression of TGF-β1, CTGF, fibronectin, COL1A1, α-SMA, and VEGF164. Compared with CG+3,4-DGE(−) mice, the CG+145 μmol/L 3,4-DGE mice showed increased TGF-β1, CTGF, fibronectin, COL1A1, α-SMA, and VEGF164 expression, suggesting that the combination of CG and 3,4-DGE enhances extracellular matrix production.

Next, we examined the expression of NOX1, NOX4, p22phox, p47phox, and gp91phox, which are essential membrane components of NAD(P)H oxidase, in peritoneum. Compared with PBS+3,4-DGE(−) mice, the PBS+38 μmol/L 3,4-DGE mice did not show increases in mRNA expression for those components. Compared with PBS+3,4-DGE(−) mice, the PBS+145 μmol/L 3,4-DGE

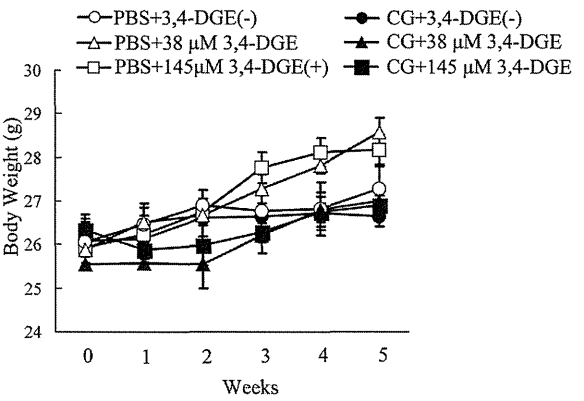

Figure 1 — Time course of body weight in mice. Mice were treated with intraperitoneal injections of 0.1% chlorhexidine gluconate (CG) or phosphate buffered saline (PBS) every other day for a week. They were then injected with 38 μmol/L or 145 μmol/L 3,4-dideoxyglucosone-3-ene (3,4-DGE) or PBS every weekday for 4 weeks. Initial PBS followed by PBS without 3,4-DGE (n = 10, open circles); initial PBS followed by PBS plus 38 μmol/L 3,4-DGE (n = 8, open triangles); initial PBS followed by PBS with 145 μmol/L 3,4-DGE (n = 5, open squares); initial CG followed by PBS without 3,4-DGE (n = 8, closed circles); initial CG followed by PBS with 38 μmol/L 3,4-DGE (n = 11, closed triangles); CG plus 145 μmol/L followed by PBS with 3,4-DGE (n = 5, close squares). All mice were compared with mice receiving PBS without 3,4-DGE; no significant differences were observed.

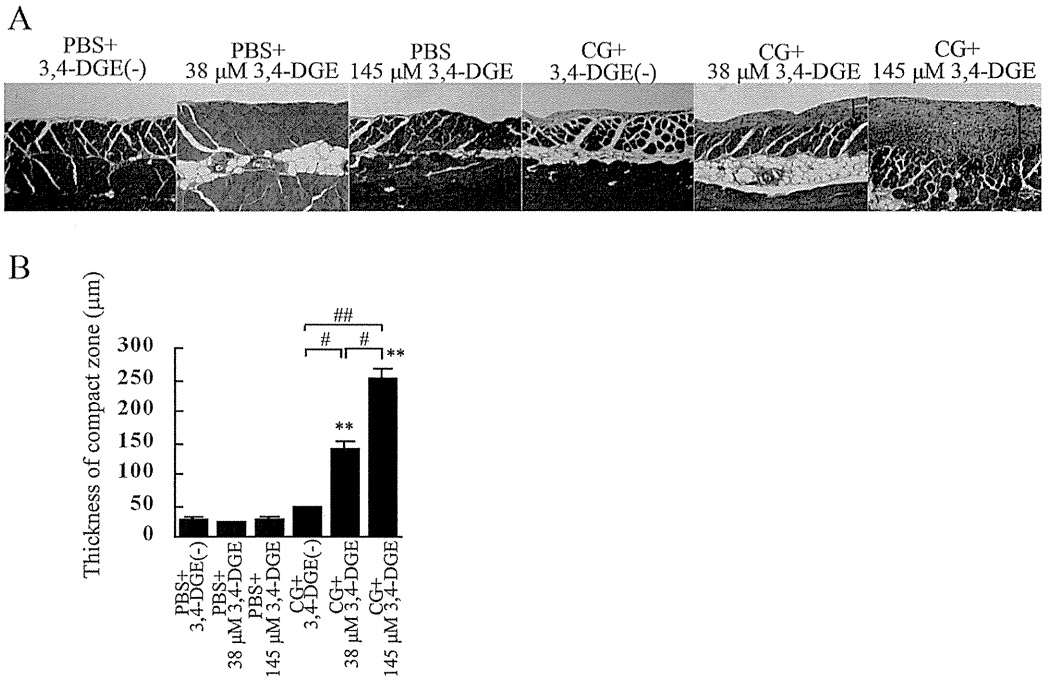

Figure 2 — Histologic appearance of the peritoneum in each group. (A) Compared with mice treated with phosphate-buffered saline (PBS) plus 38 μmol/L 3,4-dideoxyglucosone-3-ene (3,4-DGE), mice treated with chlorhexidine gluconate (CG) plus 38 μmol/L 3,4-DGE showed thickened peritoneum. In mice treated with CG+145 μmol/L 3,4-DGE, peritoneal fibrosis was more pronounced. Arrows indicate the submesothelial compact zone (Masson trichrome stain). (B) Thickness of the peritoneal membrane (mean ± standard error of the mean) in mice under various conditions: PBS without 3,4-DGE [PBS+3,4-DGE(−), $n = 7$]; PBS+38 μmol/L 3,4-DGE ($n = 5$); PBS+145 μmol/L 3,4-DGE ($n = 5$); CG+3,4-DGE(−) ($n = 5$); CG+38 μmol/L 3,4-DGE ($n = 6$); CG+145 μmol/L 3,4-DGE ($n = 5$). ** $p < 0.01$ versus mice treated with PBS and same dose of 3,4-DGE; # $p < 0.05$; ## $p < 0.01$.

mice showed increased mRNA expression of p22phox. The CG+38 μmol/L 3,4-DGE mice showed higher expression of NOX1 and NOX4 than did CG+3,4-DGE(−) mice. In CG+145 μmol/L 3,4-DGE mice, NOX4, p47phox, and gp91phox mRNA expression were higher than the expression observed in PBS+3,4-DGE(−) mice. These results suggest that the combination of CG and 3,4-DGE can increase oxidative stress.

MACROPHAGE RECRUITMENT, A-SMA–POSITIVE CELLS, AND VASCULAR VESSELS

Macrophage infiltration was assessed by immunohistochemistry for F4/80 [Figure 4(A)]. The number of macrophages in peritoneum was very small in PBS+3,4-DGE(−) and 38 μmol/L or 145 μmol/L PBS+3,4-DGE mice [Figure 4(B)]. In CG+3,4-DGE(−) mice, significantly increased numbers of F4/80-positive cells were observed around the submesothelial compact zone. Although the presence of 38 μmol/L 3,4-DGE did not change the number of infiltrating macrophages, the numbers of those cells were markedly increased in CG+145 μmol/L 3,4-DGE mice compared with CG+3,4-DGE(−) mice (85.1 ± 9.4 vs 5.8 ± 1.1). These results indicate that 3,4-DGE alone did not increase macrophage infiltration at the concentrations tested, but that 3,4-DGE augmented macrophage infiltration in the presence of pre-existing peritoneal injury.

We next examined α-SMA-positive cells using immunohistochemistry [Figure 4(A)]. The expression of α-SMA was confined to vascular smooth muscle cells in PBS-treated mice. In CG-treated mice, α-SMA–positive cells were localized in the submesothelial compact zone. The numbers of α-SMA–positive cells were significantly higher in both 38 μmol/L and 145 μmol/L CG+3,4-DGE mice than in CG+3,4-DGE(−) mice [20.2 ± 2.2 and 32 ± 4.5 vs 9.4 ± 1.4, Figure 4(C)].

To investigate vascular changes, we performed an immunohistochemical study for CD31 [Figure 4(A)]. In PBS-treated mice, no CD31-positive vessels were observed in the submesothelial layer. The CG+3,4-DGE(−) mice showed increased CD31-positive vessels in the compact zone, an increase that was further augmented in 38 μmol/L and 145 μmol/L CG+3,4-DGE mice.

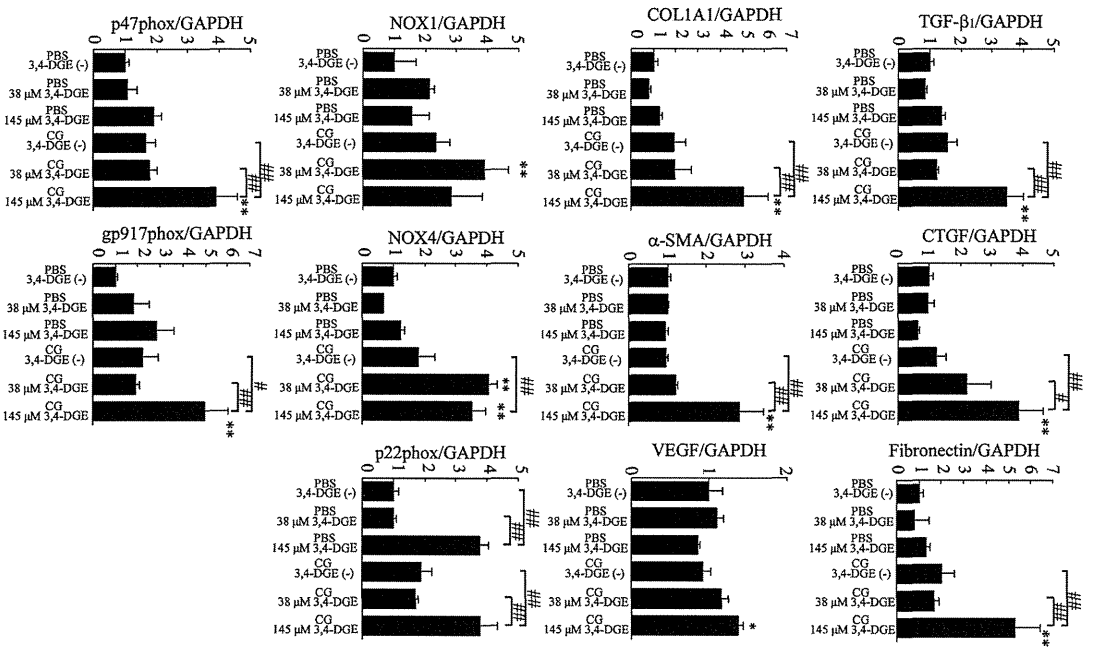

Figure 3 — Analysis by real-time reverse-transcriptase polymerase chain reaction of peritoneal expression of messenger RNA for transforming growth factor β1 (TGF-β1), connective tissue growth factor (CTGF), fibronectin, collagen type 1 α1 (COL1A1), alpha smooth muscle actin (α-SMA), vascular endothelial growth factor 164 (VEGF164), NOX1, NOX4, p22phox, p47phox, and gp91phox. GAPDH was used as a control. Number of mice: phosphate buffered saline (PBS) without 3,4-dideoxyglucosone-3-ene (3,4-DGE) ($n = 7$); PBS+38 μmol/L 3,4-DGE ($n = 5$); PBS+145 μmol/L 3,4-DGE ($n = 5$); CG without 3,4-DGE ($n = 5$); CG+38 μmol/L 3,4-DGE ($n = 6$); and CG+145 μmol/L 3,4-DGE ($n = 5$). All values: mean ± standard error of the mean. * $p < 0.05$; ** $p < 0.01$ versus mice receiving PBS with the same dose of 3,4-DGE; # $p < 0.05$; ## $p < 0.01$.

The area of CD31-positive vessels in the submesothelial compact zone was also quantified [Figure 4(D)]. The area of these blood vessels was greater in 38 μmol/L and 145 μmol/L CG+3,4-DGE mice than in CG+3,4-DGE(−) mice, and the effect was dose-dependent (1.8% ± 0.45% and 8.3% ± 1.9% vs 0.42% ± 0.11%). These results demonstrate that 3,4-DGE can increase CD31-positive vessels in injured peritoneum.

We next examined the presence of mesothelial cells by cytokeratin staining. All PBS-treated mice, including those receiving 145 μmol/L 3,4-DGE showed almost intact mesothelial cells [Figure 4(A)]. Although CG+3,4-DGE(−) mice showed no change in mesothelial cells, mice treated with of 3,4-DGE in addition to CG showed severe detachment of mesothelial cells from the peritoneal membrane [Figure 4(A)].

APOPTOSIS

We next used TUNEL staining to examine apoptosis in peritoneal injury. Almost no apoptotic cells were detected without 3,4-DGE or with 38 μmol/L 3,4-DGE even in CG-treated mice. In CG+3,4-DGE(−) mice, apoptotic cells were increased only in the abdominal rectus muscles, not in the submesothelial compact zone [Figure 5(A)]. The PBS+145 μmol/L 3,4-DGE and CG+145 μmol/L 3,4-DGE mice both showed pronounced apoptotic cells in peritoneum [Figure 5(A)].

For nuclear staining, DAPI was used. Most TUNEL-positive cells were also positive for DAPI, confirming that the TUNEL signals derived specifically from nuclei. The mean number of TUNEL-positive cells in PBS+3,4-DGE and CG+3,4-DGE mice was 3.0 and 5.9, respectively [Figure 5(B)], indicating that 3,4-DGE is relevant to apoptosis *in vivo* in the peritoneum.

To detect the cell type of the apoptotic cells, triple staining for TUNEL, DAPI, and CD45 (a leukocyte marker) was performed in CG+3,4-DGE mice [Figure 5(C)]. Some TUNEL-positive cells were positive for CD45, indicating that some of apoptotic cells were leukocytes.

ELIMINATION OF 3,4-DGE FROM THE PERITONEAL CAVITY AND APPEARANCE OF 3,4-DGE IN PLASMA

We next examined the rate at which 3,4-DGE was eliminated from the peritoneal cavity in PBS- or CG-treated